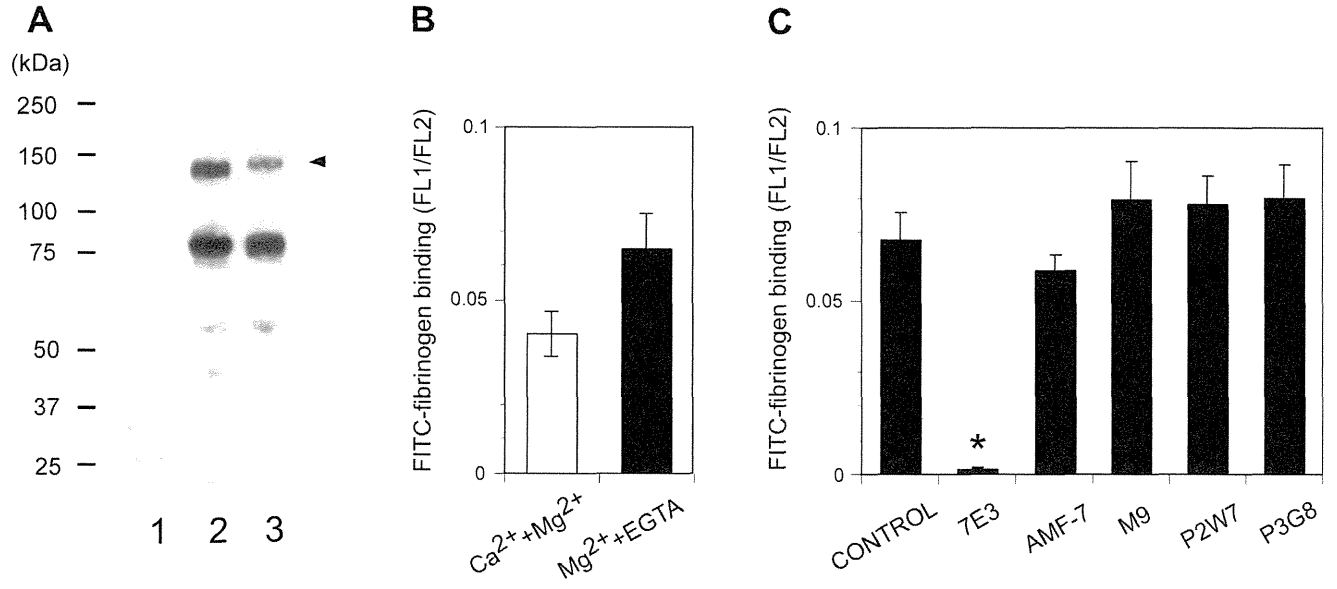

Figure 6. Effect of integrin extension on the function of the anti-αVβ3 mAbs. A. SDS-PAGE analysis of αVβ3 expressed on CHO cells. Cell lysates from biotin-labeled cells expressing αVβ3 were immunoprecipitated with anti-αV mAb P2W7. The precipitates were subjected to a 7.5% non-reducing gel and visualized using chemiluminescence. The positions of the molecular weight markers are shown on the left side of panel. Lane 1, parent CHO; lane 2, wild-type αVβ3; lane 3, Q589NAT. Note that the αV carrying the Q589NAT mutation (arrowhead) migrated more slowly than the wild type. B. FITC-fibrinogen binding to cells expressing αVβ3 carrying the Q589NAT mutation was examined as described in Fig. 4A. Binding in the presence of 1 mM Ca^{2+} and 1 mM Mg^{2+} (open column) or in the presence of 2 mM Mg^{2+} and 5 μM EGTA (solid column) is shown. C. The effect of the anti-αVβ3 mAbs on fibrinogen binding to cells expressing αVβ3 carrying the Q589NAT mutation was examined, as described in Fig. 5B. Among the mAbs, only 7E3 significantly inhibited binding.
doi:10.1371/journal.pone.0066096.g006

angle of the bend. However, we lack conclusive evidence that Q589NAT mutation actually adopts an extended conformation at this point. Although our conclusion is based on a reasonable assumption, further investigation is required to confirm our claim. Consistent with this idea, the binding interfaces of these mAbs were located close to the possible thigh/calf-1 interface in the extended conformation (Fig. 4). This mechanism might partly explain why the blocking effects of these mAbs were relatively weak compared with that of 7E3, which binds to the βA domain and inhibits ligand binding competitively [31]. Interestingly, epitope residues for an activating mAb against the α chain of αLβ2 integrin have been mapped to the back of the thigh domain, which is shielded in the bent conformation [32]. These previous results complement the present findings.

Numerous studies have shown that integrin extension is a prerequisite for integrin activation. A genetic approach in which integrin is constrained in a bent or extended conformation or in an open or closed headpiece conformation in αIIbβ3 and αLβ2 has indicated that both extension and an open headpiece are required for the binding of macromolecular ligands [6,7,13]. In agreement, another approach in which the αXβ2 conformation was constrained using functional mAbs has shown that an extended

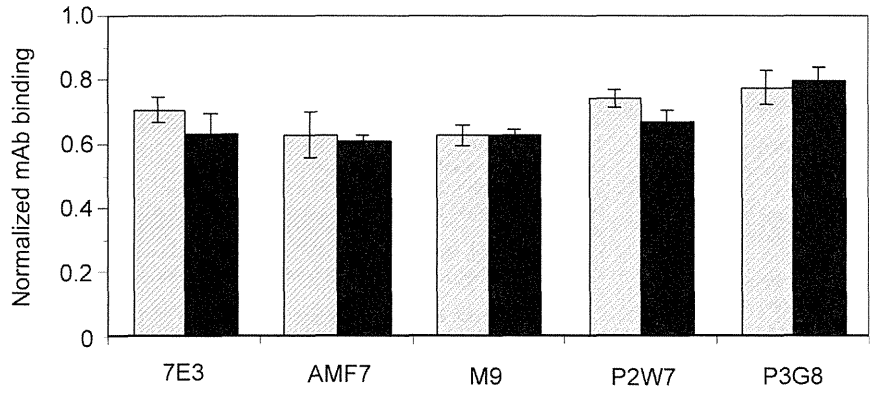

Figure 7. Effect of integrin extension on the binding of the anti-αVβ3 mAbs. Wild-type αV or αV carrying the Q589NAT mutation was transiently expressed together with wild-type β3 in CHO cells. The binding of function-blocking mAbs to these cells was examined by FACS. The MFI obtained from the whole cell population with each mAb was normalized by the MFI obtained with an anti-αV mAb 17E6 that represents the αV expression. There was no significant difference in the binding of leg-binding mAbs in cells expressing Q589NAT (solid column) as compared with cells expressing wild-type αV (hatched column).
doi:10.1371/journal.pone.0066096.g007

and open headpiece conformation represents a high-affinity state [14]. These studies clearly indicated that the extended conformation has a higher affinity for ligands than the bent conformation. Our results showed that αVβ3 was no exception. A substantial increase in fibrinogen binding was observed when αVβ3 was constrained in the extended conformation (Fig. 6B).

In contrast, several studies have suggested that the above is not true for αVβ3 integrin. Among them, the most compelling evidence showed that recombinant soluble αVβ3 could bind a fibronectin fragment while in a bent conformation [16]. This finding suggests that a bent and closed headpiece conformation represents a high-affinity state in αVβ3, which is completely opposite to the above-described results. The key to resolving this discrepancy may reside in the experimental conditions used in the experiments. As Blue et al. pointed out, whether integrin extension is required for ligand binding depends on the size of the ligand [6]. This situation probably arises because small ligands can gain access to a ligand-binding site in the proximity of the plasma membrane more easily than large ligands when the integrin is in its bent conformation. In other words, extension may regulate the accessibility of the ligand to integrin on the cell surface. If this is the case, extension might no longer be required in the absence of a plasma membrane. In agreement with this hypothesis, the recombinant αVβ3 lacked a transmembrane-cytoplasmic domain and the $FNIII_{7\text{-}10}$ fragment used in their experiment was relatively small and bound to αVβ3 at the C terminus, which would not interfere with the plasma membrane in the first place. However, considering the fact that $FNIII_{7\text{-}10}$ is located in the middle of the molecule, not at the terminus, the presence of the plasma membrane would hinder the binding of a native fibronectin molecule in the bent conformation. Thus, extension would be required for αVβ3 on the cell surface to interact with native fibronectin. Another important point is how the integrins are activated. In most experiments, Mn^{2+} is used to "activate" αVβ3 integrin. Although Mn^{2+} has been shown to induce extension in recombinant soluble αVβ3 [5], this might not be true for αVβ3 expressed on the cell surface with an intact interaction between the transmembrane-cytoplasmic domains of the α and the β subunits. Consistent with this idea, the height of αIIbβ3 reconstituted in liposomes did not change after Mn^{2+} activation [33]. In our experiments, the expression of an anti-LIBS epitope, which is preferentially expressed in liganded integrins, was not observed after Mn^{2+} activation, suggesting that extensive structural rearrangement did not occur because of Mn^{2+} alone (unpublished data). A comparison of the crystal structures of liganded and unliganded αVβ3 has revealed that the rearrangement of the cation/ligand binding sites occurs without a swing-out in the presence of Mn^{2+} [2,15]. A similar rearrangement was accompanied by the swing-out of the hybrid domain in a liganded αIIbβ3 headpiece that lacked the lower leg region in the presence of Ca^{2+}/Mg^{2+} [3]. These results suggest that although an open headpiece conformation might be required for activation in Ca^{2+}/Mg^{2+}, such a conformation might not be necessary in Mn^{2+}. If this is the case, a bent and closed headpiece conformation could bind macromolecular ligands as long as the proximity of the plasma membrane did not prevent ligand access. Thus, integrins could bind ligands in the bent and closed headpiece conformation under specific experimental conditions. However, in physiological settings, extension and open headpiece conformation are both indispensable for high-affinity ligand interactions. It would be interesting to examine whether a closed headpiece conformer binds ligand in the presence of Mn^{2+}. In addition, the direct interaction of a soluble bent conformer with a ligand would have to be established to substantiate the hypothesis described above.

Our results and those of others indicate that the extended conformation has a higher affinity for ligands than the bent conformation, and nothing more. Although integrins fixed in a completely bent or extended conformation can be engineered and examined, the intermediate conformations between these two extremes are difficult to recreate experimentally. For this reason, no information is available regarding how much extension is needed to allow ligand binding. In other words, complete extension may not be necessary for initial ligand binding. This idea may explain why no substantial differences in the fluorescent donor-accepter separation distance between the fluorescent dye-labeled membrane and the fluorescent dye-labeled mAb bound to the β-propeller domain were detected between wild-type and a constitutively active mutant of αVβ3 [17]. Instead, an external force applied to the head region may be required to accomplish extension, as simulations of the molecular dynamics of αVβ3 have suggested [34]. Such forced extension may greatly stabilize integrin-ligand interactions [35]. Taken together, the present findings suggest that the switchblade-like movement of the integrin leg regulates the αVβ3-ligand interaction.

Author Contributions

Conceived and designed the experiments: TK. Performed the experiments: ST YS. Analyzed the data: TK SA. Contributed reagents/materials/analysis tools: MH YK YI. Wrote the paper: TK.

References

1. Hynes RO (2002) Integrins: bidirectional, allosteric signaling machines. Cell 110: 673–687.
2. Xiong JP, Stehle T, Diefenbach B, Zhang R, Dunker R, et al. (2001) Crystal structure of the extracellular segment of integrin alpha Vbeta3. Science 294: 339–345.
3. Xiao T, Takagi J, Coller BS, Wang JH, Springer TA (2004) Structural basis for allostery in integrins and binding to fibrinogen-mimetic therapeutics. Nature 432: 59–67.
4. Weisel JW, Nagaswami C, Vilaire G, Bennett JS (1992) Examination of the platelet membrane glycoprotein IIb-IIIa complex and its interaction with fibrinogen and other ligands by electron microscopy. J Biol Chem 267: 16637–16643.
5. Takagi J, Petre BM, Walz T, Springer TA (2002) Global conformational rearrangements in integrin extracellular domains in outside-in and inside-out signaling. Cell 110: 599–511.
6. Blue R, Li J, Steinberger J, Murcia M, Filizola M, et al. (2010) Effects of limiting extension at the alphaIIb genu on ligand binding to integrin alphaIIbbeta3. J Biol Chem 285: 17604–17613.
7. Kamata T, Handa M, Ito S, Sato Y, Ohtani T, et al. (2010) Structural requirements for activation in alphaIIb beta3 integrin. J Biol Chem 285: 38428–38437.
8. Ye F, Hu G, Taylor D, Ratnikov B, Bobkov AA, et al. (2010) Recreation of the terminal events in physiological integrin activation. J Cell Biol 188: 157–173.
9. Takagi J, Strokovich K, Springer TA, Walz T (2003) Structure of integrin alpha5beta1 in complex with fibronectin. Embo J 22: 4607–4615.
10. Springer TA, Zhu J, Xiao T (2008) Structural basis for distinctive recognition of fibrinogen gammaC peptide by the platelet integrin alphaIIbbeta3. J Cell Biol 182: 791–800.
11. Luo BH, Takagi J, Springer TA (2004) Locking the beta3 integrin I-like domain into high and low affinity conformations with disulfides. J Biol Chem 279: 10215–10221.
12. Luo BH, Strokovich K, Walz T, Springer TA, Takagi J (2004) Allosteric beta1 integrin antibodies that stabilize the low affinity state by preventing the swing-out of the hybrid domain. J Biol Chem 279: 27466–27471.
13. Tang XY, Li YF, Tan SM (2008) Intercellular adhesion molecule-3 binding of integrin alphaL beta2 requires both extension and opening of the integrin headpiece. J Immunol 180: 4793–4804.
14. Chen X, Xie C, Nishida N, Li Z, Walz T, et al. (2010) Requirement of open headpiece conformation for activation of leukocyte integrin alphaXbeta2. Proc Natl Acad Sci U S A 107: 14727–14732.
15. Xiong JP, Stehle T, Zhang R, Joachimiak A, Frech M, et al. (2002) Crystal structure of the extracellular segment of integrin alpha Vbeta3 in complex with an Arg-Gly-Asp ligand. Science 296: 151–155.

16. Adair BD, Xiong JP, Maddock C, Goodman SL, Arnaout MA, et al. (2005) Three-dimensional EM structure of the ectodomain of integrin {alpha}V{-beta}3 in a complex with fibronectin. J Cell Biol 168: 1109–1118.
17. Xiong JP, Mahalingham B, Alonso JL, Borrelli LA, Rui X, et al. (2009) Crystal structure of the complete integrin alphaVbeta3 ectodomain plus an alpha/beta transmembrane fragment. J Cell Biol 186: 589–600.
18. Tokuhira M, Handa M, Kamata T, Oda A, Katayama M, et al. (1996) A novel regulatory epitope defined by a murine monoclonal antibody to the platelet GPIIb-IIIa complex (alpha IIb beta 3 integrin). Thromb Haemost 76: 1038–1046.
19. de Vries JE, Keizer GD, te Velde AA, Voordouw A, Ruiter D, et al. (1986) Characterization of melanoma-associated surface antigens involved in the adhesion and motility of human melanoma cells. Int J Cancer 38: 465–473.
20. Lehmann M, Rabenandrasana C, Tamura R, Lissitzky JC, Quaranta V, et al. (1994) A monoclonal antibody inhibits adhesion to fibronectin and vitronectin of a colon carcinoma cell line and recognizes the integrins alpha v beta 3, alpha v beta 5, and alpha v beta 6. Cancer Res 54: 2102 2107.
21. Mitjans F, Sander D, Adan J, Sutter A, Martinez JM, et al. (1995) An anti-alpha v-integrin antibody that blocks integrin function inhibits the development of a human melanoma in nude mice. J Cell Sci 108 (Pt 8): 2825–2838.
22. von Schlippe M, Marshall JF, Perry P, Stone M, Zhu AJ, et al. (2000) Functional interaction between E-cadherin and alphav-containing integrins in carcinoma cells. J Cell Sci 113 (Pt 3): 425 437.
23. Wayner EA, Orlando RA, Cheresh DA (1991) Integrins alpha v beta 3 and alpha v beta 5 contribute to cell attachment to vitronectin but differentially distribute on the cell surface. J Cell Biol 113: 919–929.
24. Friedlander DR, Zagzag D, Shiff B, Cohen H, Allen JC, et al. (1996) Migration of brain tumor cells on extracellular matrix proteins in vitro correlates with tumor type and grade and involves alphaV and beta1 integrins. Cancer Res 56: 1939–1947.
25. Cheresh DA (1987) Human endothelial cells synthesize and express an Arg-Gly-Asp-directed adhesion receptor involved in attachment to fibrinogen and von Willebrand factor. Proc Natl Acad Sci U S A 84: 6471–6475.
26. Horton MA, Lewis D, McNulty K, Pringle JA, Chambers TJ (1985) Monoclonal antibodies to osteoclastomas (giant cell bone tumors): definition of osteoclast-specific cellular antigens. Cancer Res 45: 5663 5669.
27. Coller BS (1985) A new murine monoclonal antibody reports an activation-dependent change in the conformation and/or microenvironment of the platelet glycoprotein IIb/IIIa complex. J Clin Invest 76: 101–108.
28. Chuntharapai A, Bodary S, Horton M, Kim KJ (1993) Blocking monoclonal antibodies to alpha V beta 3 integrin: a unique epitope of alpha V beta 3 integrin is present on human osteoclasts. Exp Cell Res 205: 345–352.
29. Kamata T, Handa M, Sato Y, Ikeda Y, Aiso S (2005) Membrane-proximal {alpha}/{beta} stalk interactions differentially regulate integrin activation. J Biol Chem 280: 24775–24783.
30. Kamata T, Irie A, Tokuhira M, Takada Y (1996) Critical residues of integrin alphaIIb subunit for binding of alphaIIbbeta3 (glycoprotein IIb-IIIa) to fibrinogen and ligand-mimetic antibodies (PAC-1, OP-G2, and LJ-CP3). J Biol Chem 271: 18610–18615.
31. Puzon-McLaughlin W, Kamata T, Takada Y (2000) Multiple discontinuous ligand-mimetic antibody binding sites define a ligand binding pocket in integrin alpha(IIb)beta(3). J Biol Chem 275: 7795–7802.
32. Xie C, Shimaoka M, Xiao T, Schwab P, Klickstein LB, et al. (2004) The integrin alpha-subunit leg extends at a Ca2+-dependent epitope in the thigh/genu interface upon activation. Proc Natl Acad Sci U S A 101: 15422–15427.
33. Ye F, Liu J, Winkler H, Taylor KA (2008) Integrin alpha IIb beta 3 in a membrane environment remains the same height after Mn2+ activation when observed by cryoelectron tomography. J Mol Biol 378: 976–986.
34. Chen W, Lou J, Hsin J, Schulten K, Harvey SC, et al. (2011) Molecular dynamics simulations of forced unbending of integrin alpha(v)beta(3). PLoS Comput Biol 7: e1001086.
35. Litvinov RI, Mekler A, Shuman H, Bennett JS, Barsegov V, et al. (2012) Resolving two-dimensional kinetics of the integrin alphaIIbbeta3-fibrinogen interactions using Binding-Unbinding Correlation Spectroscopy. J Biol Chem.

Pharmacokinetic Study of Adenosine Diphosphate-Encapsulated Liposomes Coated with Fibrinogen γ-Chain Dodecapeptide as a Synthetic Platelet Substitute in an Anticancer Drug-Induced Thrombocytopenia Rat Model

KAZUAKI TAGUCHI,[1,5] HAYATO UJIHIRA,[1] HIROSHI WATANABE,[1,2] ATSUSHI FUJIYAMA,[3] MAMI DOI,[3] SHINJI TAKEOKA,[3] YASUO IKEDA,[3] MAKOTO HANDA,[4] MASAKI OTAGIRI,[1,5,6] TORU MARUYAMA[1,2]

[1]Department of Biopharmaceutics, Graduate School of Pharmaceutical Sciences, Kumamoto University, Chuo-ku, Kumamoto, 862–0973, Japan

[2]Center for Clinical Pharmaceutical Sciences, Kumamoto University, Chuo-ku, Kumamoto, 862–0973, Japan

[3]Department of Life Science and Medical Bioscience, Graduate School of Advanced Science and Engineering, Waseda University, Wakamatsu, Shinjuku-ku, Tokyo, 162–8480, Japan

[4]Department of Transfusion Medicine & Cell Therapy, Keio University, Shinjuku-ku, Tokyo, 160–8582, Japan

[5]Faculty of Pharmaceutical Sciences, Sojo University, Nishi-ku, Kumamoto, 862–0082, Japan

[6]DDS Research Institute, Sojo University, Nishi-ku, Kumamoto, 862–0082, Japan

Received 14 June 2013; revised 3 July 2013; accepted 17 July 2013

Published online 5 August 2013 in Wiley Online Library (wileyonlinelibrary.com). DOI 10.1002/JPS.23692

ABSTRACT: A fibrinogen γ-chain (dodecapeptide HHLGGAKQAGDV, H12)-coated, adenosine diphosphate (ADP)-encapsulated liposome [H12-(ADP)-liposome] was designed to achieve optimal performance as a homeostatic agent and expected as a synthetic platelet alternative. For the purpose of efficient function as platelet substitute, H12-(ADP)-liposomes should potentially have both acceptable pharmacokinetic and biodegradable properties under conditions of an adaptation disease including thrombocytopenia induced by anticancer drugs. The aim of this study was to characterize the pharmacokinetics of H12-(ADP)-liposomes in busulphan-induced thrombocytopenic rats using ^{14}C, ^{3}H double radiolabeled H12-(ADP)-liposomes, in which the encapsulated ADP and liposomal membrane (cholesterol) were labeled with ^{14}C and ^{3}H, respectively. After the administration of H12-(ADP)-liposomes, they were determined to be mainly distributed to the liver and spleen and disappeared from organs within 7 days after injection. The encapsulated ADP was mainly eliminated in the urine, whereas the outer membrane (cholesterol) was mainly eliminated in feces. The successive dispositions of the H12-(ADP)-liposomes were similar in both normal and thrombocytopenic rats. However, the kinetics of H12-(ADP)-liposomes in thrombocytopenic rats was more rapid, compared with the corresponding values for normal rats. These findings, which well reflect the clinical features of patients with anticancer drug-induced thrombocytopenia, provide useful information for the development of the H12-(ADP)-liposomes for future clinical use. © 2013 Wiley Periodicals, Inc. and the American Pharmacists Association J Pharm Sci 102:3852–3859, 2013

Keywords: liposome; adenosine-diphosphate; dodecapeptide; disposition; thrombocytopenia; platelet substitute; biocompatibility; disease state; cancer chemothrapy

INTRODUCTION

Platelet transfusion represents one of the most essential prophylactic or therapeutic treatments for patients with thrombocytopenia caused by hematologic malignancies, or caused as a result of intensive chemotherapy and radiation used in the treatment of solid tumors. However, platelet transfusion can introduce a variety of complications such as virus infections, allergic reactions, and acute lung injuries. In addition, the shortage of donated platelets for blood transfusions has also become a serious issue because of the short shelf life of such products (4 days in Japan and 5–7 days in the USA and Europe) and our aging society and the need for a stable supply in an emergency situation such as disasters and pandemics. To overcome these problems, attempts have been made to develop various platelet substitutes (artificial platelets), which consist of materials derived from blood components,[1] such as solubilized platelet membrane protein-conjugated liposomes (plateletsome),[2] infusible platelet membranes,[3] fibrinogen-coated albumin microcapsules (synthocyte),[4] red blood cells (RBC) with bound fibrinogen,[5] liposomes bearing fibrinogen,[6] arginine-glycine-aspartic acid peptide-bound RBC (Thromboerythrocyte)[7] and fibrinogen-conjugated albumin polymers.[8]

Adenosine diphosphate (ADP)-encapsulated liposomes modified with a dodecapeptide (^{400}HHLGGAKQAGDV^{411}, H12) in the carboxy terminus of the fibrinogen γ-chain [H12-(ADP)-liposome] were developed as a new type of synthetic platelet alternative. The modification of H12-(ADP)-liposomes such as H12 and encapsulation with ADP enable them to specifically interact with activated platelets and stimulate platelet aggregation. It is well known that H12-(ADP)-liposomes bind to

Abbreviations used: ADP, adenosine diphosphate; H12, dodecapeptide (^{400}HHLGGAKQAGDV^{411}); AST, aspartate aminotransferase; ALT, alanine aminotransferase; BUN, blood urea nitrogen; CRE, creatinine; $t_{1/2}$, half-life; MRT, mean residence time; AUC, area under the concentration–time curve; CL, clearance; V_{dss}, distribution volume; MCV, mean corpuscular volume; MCH, mean corpuscular hemoglobin; MCHC, mean corpuscular hemoglobin concentration; HbV, hemoglobin vesicles; MPS mononuclear phagocyte system.

Correspondence to: Toru Maruyama (Telephone: +81-96-361-4150; Fax: +81-96-362-7690; E-mail: tomaru@gpo.kumamoto-u.ac.jp)

Journal of Pharmaceutical Sciences, Vol. 102, 3852–3859 (2013)

glycoprotein IIb/IIIa on activated platelet membranes and accumulate between adherent platelets, analogous to fibrinogen in *in vitro* studies.[9–11] Furthermore, it was also reported that H12-(ADP)-liposomes specifically accumulate at the site of an injury *in vivo* and were reported to decrease bleeding time in a dose-dependent manner in both thrombocytopenic rat and rabbit models.[12–16] On the basis of these findings, it would be reasonable to conclude that H12-(ADP)-liposomes may be clinically acceptable for several disorders, such as injury, acute thrombocytopenic trauma with massive bleeding, and thrombocytopenia induced by drugs, as a platelet alterative.

Before new drugs are approved for clinical use, they are required to undergo a wide variety of evaluations, including physicochemical tests, preclinical studies, and clinical trials. Despite the accumulated basic evidence for the pharmacological effectiveness of H12-(ADP)-liposomes in the preclinical stage,[12–16] the pharmacokinetics of H12-(ADP)-liposomes have not been well characterized. Pharmacokinetic studies of H12-(ADP)-liposomes that have been reported to date have evaluated only their dispositions in normal animals including mice, rats, and rabbits.[17] In previous studies, it was reported that clinical conditions can affect the pharmacokinetics of liposomes.[18–20] Furthermore, Frank and Hargreaves reported that safe/toxicology and pharmacokinetic data, which are used to estimate pharmacokinetic studies in preclinical stages, accounts for approximately 40% of the failed attempts to develop new drug projects during clinical development.[21] Therefore, clarifying the pharmacokinetics of H12-(ADP)-liposomes in animal models of an adaptation disease (thrombocytopenia) should provide useful information, such as dosing regimens required for future clinical applications. In addition, the characteristics of the H12-(ADP)-liposomes developed in this study suggest that not only better pharmacological effects could be obtained, but the product may well have acceptable biodegradable properties (no accumulation or retention). These effects, however, need to be documented even under conditions of an adaptation disease (thrombocytopenia).

In the present study, we report on an evaluation of the pharmacokinetic properties of H12-(ADP)-liposomes and components derived from them in thrombocytopenia model rats produced as the result of anticancer drug therapy, which is a candidate for a disease that could be treated with H12-(ADP)-liposomes. For this purpose, we first created thrombocytopenia model rats induced by treatment with busulphan, anticancer drug used in the treatment of hematologic malignancies. We then evaluated the pharmacokinetic properties of the H12-(ADP)-liposomes and components in the thrombocytopenia model rats using ^{14}C, ^{3}H double radiolabeled H12-(ADP)-liposomes, in which the encapsulated ADP and membrane component (cholesterol) were labeled with ^{14}C and ^{3}H, respectively, and subsequently compared with the findings for those obtained using normal rats.

MATERIALS AND METHODS

Reagents

Cholesterol and 1,2-dipalmitoyl-*sn*-glycero-3-phosphatidylcholine were purchased from Nippon Fine Chemical (Osaka, Japan), and 2-distearoyl-*sn*-glycero-3-phosphatidylethanolamine-N-[monomethoxypoly(ethyleneglycol)] (5.1 kDa) was purchased from NOF (Tokyo, Japan). 1,5-Dihexadecyl-*N*-succinyl-L-glutamate and H12–polyethyleneglycol (PEG)–Glu2C18, in which the fibrinogen γ-chain dodecapeptide (C-HHLGGAKQAGDV, Cys–H12) was conjugated to the end of the PEG–lipids, were synthesized as reported previously.[15] Busulphan was obtained from Sigma–Aldrich (St Louis, Missouri).

Animals

All animal experiments were undertaken in accordance with the guidelines, principles, and procedures of Kumamoto University for the care and use of laboratory animals. Experiments were carried out with male Sprague–Dawley rats (Kyudou Company, Kumamoto, Japan). All animals were maintained under conventional housing conditions, with food and water *ad libitum* in a temperature-controlled room with a 12-h dark/light cycle.

Preparation of Thrombocytopenic Rats

Thrombocytopenic rats induced by busulphan were created as previously reported by Yang et al.[22] with minor modifications. Typically, a busulphan solution was prepared at a final concentration of 10 mg/mL in PEG (average molecular weight 400). Rats were anaesthetized with ether and intraperitoneally injected on days 0 and 3 with equal amounts of a total dose of busulphan of 20 mg/kg.

Blood Sampling, Measurement of Hematology, and Serum Chemistry

At stipulated dates (0–14th day, 16th day, 18th day, and 20th day) after busulphan administration, blood samples (approximately 100 μL) for cell counts were obtained from the tail veins of ether-anaesthetized rats. Hematology analyses of venous samples were performed using KX-21NV (Sysmex, Kobe, Japan). The remaining venous blood samples obtained at days 0 and 10 after busulphan administration were centrifuged (1710*g*, 10 min) to obtain serum, which was used for the evaluation of serum chemistry [aspartate aminotransferase (AST), alanine aminotransferase (ALT), blood urea nitrogen (BUN), and creatinine]. AST and ALT activities levels were determined by using a transaminase C-II test kit from Wako Chemicals (Saitama, Japan). BUN and creatinine were determined by using a urea nitrogen-B test kit and LabAssay creatinine test kit from Wako Chemicals, respectively.

Preparation of ^{14}C, ^{3}H Double-Labeled H12-(ADP)-Liposomes

^{14}C-labeled H12-(ADP)-liposomes were first prepared under sterile conditions, as previously reported.[16] The diameter and Zeta potential of the ^{14}C-labeled H12-(ADP)-liposomes used in this study are regulated at 250 ± 50 nm and − 10 ± 0.9 mV, respectively. The ^{3}H labeling of ^{14}C-labeled H12-(ADP)-liposomes was carried out according to a previous report.[17] Before being used in pharmacokinetic experiments, all of the samples were mixed with unlabeled H12-(ADP)-liposomes.

Pharmacokinetic Studies in Thrombocytopenic Rats

Ten days after the administration of busulphan, 16 thrombocytopenic rats were anesthetized with ether and given a single injection of ^{14}C, ^{3}H-labeled H12-(ADP)-liposomes (10 mg lipids/kg). In all rat groups, four rats were selected to undergo a plasma concentration test. Under ether anesthesia,

approximately 200 μL blood sample from all administered groups were collected from the tail vein at multiple time points after the injection of the ^{14}C, ^{3}H-labeled H12-(ADP)-liposomes (3, 10, and 30 min; 1, 2, 3, 6, 12, and 24 h), and the plasma was separated by centrifugation (3000*g*, 5 min). After collecting the last blood sample (24 h), the rats were sacrificed and selected organs (kidney, liver, spleen, lung, and heart) were excised. Urine and feces were collected at fixed intervals in a metabolic cage. In addition, the four thrombocytopenic rats were randomly sacrificed and organs (kidney, liver, spleen, lung, and heart) were collected at 2 and 6 h and 7 days after an injection of ^{14}C, ^{3}H-labeled H12-(ADP)-liposomes at a dose of 10 mg lipids/kg.

Measurement of ^{14}C and ^{3}H Radioactivity

Plasma samples were solubilized in a mixture of Soluene-350 (Perkin Elmer, Yokohama, Japan) and isopropyl alcohol (at a ratio of 1/1) for 24 h at 50°C. The organ samples were rinsed with saline, minced, and solubilized in Soluene-350 for 24 h at 50°C. Urine and feces were also weighed and solubilized in Soluene-350. All samples were decolorized by treatment with a hydrogen peroxide solution after the Soluene-350 or isopropyl alcohol treatments. The ^{14}C, ^{3}H radioactivity was determined by liquid scintillation counting (LSC-5121; Aloka, Tokyo, Japan) with Hionic Fluor (Perkin Elmer).

Data Analysis

A noncompartment model was used for the pharmacokinetic analysis. Each parameter, half-life ($t_{1/2}$, h), mean residence time (h), area under the concentration–time curve (AUC, h % of dose/mL), clearance (CL, mL/h), distribution volume (mL), was calculated using the moment analysis program available on Microsoft Excel.[23] Data are shown as the mean ± SD for the indicated number of animals.

RESULTS AND DISCUSSION

The Creation of Thrombocytopenic Rats Induced by Busulphan

All rats survived the busulphan treatment and none were on the verge of death. Although the body weight of nontreatment rats were increased from 236.7 ± 5.8 to 310.6 ± 13.3 g, the weights of the busulphan-administered rats (thrombocytopenic rats) were only increased slightly, from 235.0 ± 4.2 to 289.5 ± 9.3 g at 10 days after busulphan administration.

Platelet counts of the rats that had been treated with busulphan were 91.0 ± 5.8 × 10^4 per microliter before busulphan administration, and declined significantly to 27.7 ± 2.7 × 10^4 per microliter at 10 days after busulphan administration, which meets the clinical criterion for thrombocytopenia (Fig. 1c). This severe thrombocytopenia was consistent with results reported in previous studies for busulphan treated rats at 10 days after busulphan administration.[14,16] Furthermore, the number of white blood cells and RBC slowly begun to decrease from 1 day after busulphan administration (Figs. 1a and 1b). In association with the decrease in RBC, the hemoglobin and hematocrit values were also altered (Table 1). However, the RBC-related parameters, including the mean corpuscular volume, mean corpuscular hemoglobin, and mean corpuscular hemoglobin concentration were not changed between before busulphan administration and 10 day after busulphan administration (Table 1). These results indicate that thrombocytopenia model rats are associated with the adverse effect (pancytopenia) of busulphan.

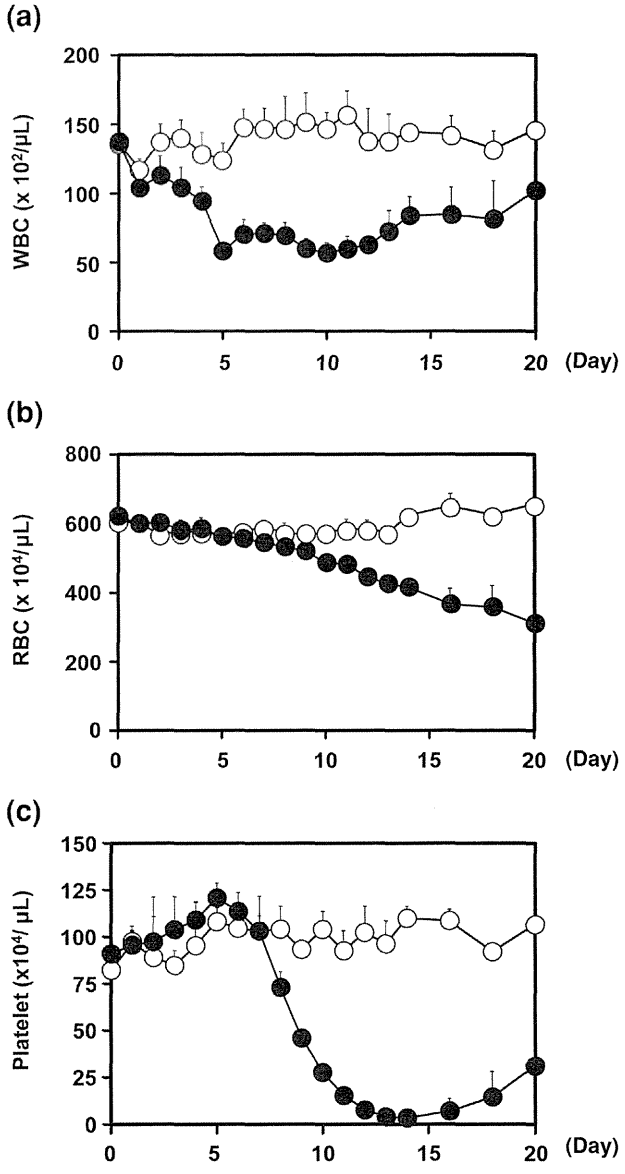

Figure 1. Time course for number of white blood cell (a), red blood cell (b), and platelet (c) in normal rats (open circle) and rats treated by busulphan at a total dose of 20 mg/kg (closed circle). Busulphan was interperitoneally injected to rats on days 0 and 3 with equal amounts of a total dose of busulphan of 20 mg/kg. Each point represents the mean ± SD ($n = 4$).

In clinical situations, patients with cancer, such as hematologic malignancies, receiving anticancer drugs frequently, need therapeutic platelet transfusions to counteract the effects of the anticancer drugs. Busulphan, one of the anticancer drugs used in the treatment of hematologic malignancies, induces thrombocytopenia as an adverse effect. Furthermore, the putative strategy for using H12-(ADP)-liposomes in a clinical situation is to alleviate the thrombocytopenia induced by anticancer drugs. Taken together, the rat model of thrombocytopenia created in the present study acceptably reflects this clinical situation. Therefore, a pharmacokinetic study of H12-(ADP)-liposomes was performed using busulphan-induced thrombocytopenia model rats at 10 days after busulphan administration.

DOI 10.1002/JPS.23692

Table 1. Changes in Hemoglobin, Hematocrit, and Other Red Blood Cells-Related Parameters in Normal Rats and Thrombocytopenic Rats at 0 and 10 Days After Busulphan Administration

	Nontreatment Rats		Thrombocytopenia Rats	
	Day (0)	Day (10)	Day (0)	Day (10)
Hemoglobin (g/dL)	13.1 ± 0.3	13.3 ± 1.4	13.5 ± 0.3	11.1 ± 0.2
Hematocrit (%)	39.2 ± 0.4	37.9 ± 0.3	40.5 ± 0.9	32.6 ± 0.7
MCV (fL)	71.0 ± 1.7	72.5 ± 1.0	71.6 ± 1.0	73.7 ± 0.8
MCH (pg)	23.7 ± 0.9	24.2 ± 0.2	24.0 ± 0.4	25.1 ± 0.4
MCHC (g/dL)	36.7 ± 1.2	36.7 ± 0.4	36.8 ± 0.3	37.3 ± 0.7

Blood samples (~100 μL) for cell counts were obtained from ether-anaesthetized rats treated with or without busulphan from a tail vein. Red blood cells-related parameters of venous samples were analyzed using automated blood cell counter.

Each value represents the mean ± SD ($n = 4$).

MCV, mean corpuscular volume; MCH, mean corpuscular hemoglobin; MCHC, mean corpuscular hemoglobin concentration.

Table 2. Serum Biochemical Parameters Representing Hepatic and Renal Function in Normal Rats and Thrombocytopenic Rats at 0 and 10 Days After Busulphan Administration

	Nontreatment Rats		Thrombocytopenia Rats	
	Day (0)	Day (10)	Day (0)	Day (10)
AST (IU/L)	32.0 ± 3.2	41.0 ± 5.6	31.0 ± 1.8	27.8 ± 3.3
ALT (IU/L)	8.2 ± 2.2	12.2 ± 1.1	7.7 ± 2.2	12.5 ± 1.6
CRE (mg/dL)	0.91 ± 0.05	1.08 ± 0.22	0.93 ± 0.17	0.90 ± 0.13
BUN (mg/dL)	15.7 ± 0.5	15.1 ± 0.8	17.2 ± 3.1	16.6 ± 3.1

Each value represents the mean ± SD ($n = 4$).

AST, aspartate aminotransferase; ALT, alanine aminotransferase; CRE, creatinine; BUN, blood urea nitrogen.

Serum Chemistry

It is well known that hepatic and renal function can have an effect on the pharmacokinetics of hepatic and renal clearing drugs, including liposomes. For example, the pharmacokinetics of hemoglobin vesicles (HbV), the liposomal characteristics of which are similar in terms of the liposomal structure to H12-(ADP)-liposomes, were reported to be altered in a rat model of chronic liver cirrhosis.[24] Our previous report demonstrated that the ADP encapsulated in H12-(ADP)-liposomes was mainly eliminated in the urine after being metabolized to allantoin, whereas the lipid components (cholesterol) were mainly eliminated in feces via bile.[17] Therefore, it is important to consider the effect of busulphan administration on hepatic and renal function before collecting pharmacokinetic data for thrombocytopenic rats induced by busulphan treatment.

In the present study, no changes in the parameters reflecting liver function (AST and ALT) were found at 10 days after busulphan administration (Table 2). In addition, BUN and creatinine levels, which reflect renal function, were also unchanged at 10 days after busulphan administration (Table 2). These results indicate that busulphan administration had no effect on the pharmacokinetics of H12-(ADP)-liposome with respect to changes in hepatic and renal function in busulphan-induced thrombocytopenia model rats.

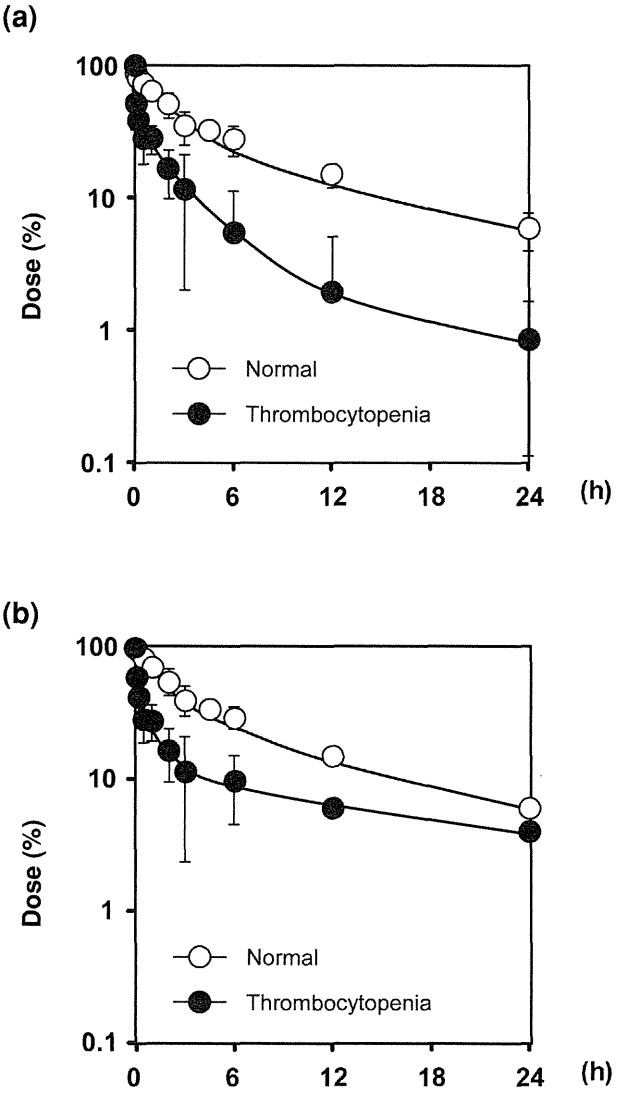

Figure 2. Plasma concentration curve of (a) ^{14}C and (b) 3H radiolabeled H12-(ADP)-liposome after intravenous injection at a dose of 10 mg lipids/kg to normal rats (open circle) and thrombocytopenic rats (closed circle). The data for the normal rats were cited from our previously reported paper.[17] Each point represents the mean ± SD ($n = 4$).

Pharmacokinetics of H12-(ADP)-Liposome Components in Normal and Thrombocytopenic Rats

Plasma Concentration

Figure 2 shows the time course for the plasma concentration of the ^{14}C, ^{3}H-labeled H12-(ADP)-liposomes that were injected into normal rats and thrombocytopenic rats at a dose of 10 mg lipid/kg, which was lowest recommended dosage to exert enough hematostatic effect in thrombocytopenic rats,[14,16] and Table 3 lists the pharmacokinetic parameters calculated from the data shown in Figure 2. The plasma concentration curves and pharmacokinetic parameters for ^{14}C radioactivity and ^{3}H radioactivity were different between normal rats and thrombocytopenic rats (Fig. 2 and Table 3). Accompanied by the change of plasma concentration curve, the $t_{1/2}$ for both ^{14}C radioactivity and ^{3}H radioactivity in thrombocytopenic rats

Table 3. The Pharmacokinetic Parameters of Inner ADP [(8C–^{14}C)ADP] and Outer Lipids Membranes [(1,2-^{3}H(N)-cholesterol)] Derived from 3H, ^{14}C Radiolabeled H12-(ADP)-Liposomes After an Intravenous Injection at a Dose of 10 mg Lipids/kg to Normal Rats and Thrombocytopenic Rats

	Normal Rats		Thrombocytopenic Rats	
	^{3}H	^{14}C	^{3}H	^{14}C
$t_{1/2}$ (h)	8.18 ± 0.77	8.21 ± 1.01	1.81 ± 0.39**	1.68 ± 0.78**
MRT (h)	10.2 ± 1.18	10.4 ± 1.46	2.17 ± 0.71**	2.09 ± 1.01**
AUC (h % of dose/mL)	58.4 ± 6.5	54.2 ± 10.1	10.7 ± 4.1**	10.2 ± 4.3**
CL (mL/h)	1.73 ± 0.18	1.89 ± 0.32	10.4 ± 4.2**	11.4 ± 5.4**
V_{dss} (mL)	17.7 ± 3.5	19.5 ± 3.6	20.7 ± 2.9	20.2 ± 1.9

The data for the normal rats were cited from our previously reported paper.[17]
**$p < 0.01$ versus normal rats.
Each value represents the mean ± SD ($n = 4$).
$t_{1/2}$, half-life; MRT, mean residence time; AUC, area under the concentration–time curve; CL, clearance; V_{dss}, distribution volume.

was approximately four times shorter than that in normal rats (^{14}C; 8.21 ± 1.01 and 1.68 ± 0.78 h, ^{3}H; 8.18 ± 0.77 and 1.81 ± 0.39 h, for normal and thrombocytopenic rats, respectively). In addition, CL in thrombocytopenic rats was increased compared with normal rats (^{14}C; 1.89 ± 0.32 and 11.4 ± 5.4 mL/h, ^{3}H; 1.73 ± 0.18 and 10.4 ± 4.2 mL/h, for normal and thrombocytopenic rats, respectively), and the AUC was decreased in the case of the thrombocytopenic rats compared with the normal rats (^{14}C; 54.2 ± 10.1 and 10.2 ± 4.3 h % of dose/mL, ^{3}H; 58.4 ± 6.5 and 10.7 ± 4.1 h % of dose/mL, for normal and thrombocytopenic rats, respectively). Interestingly, although the plasma concentration curves for ^{14}C, ^{3}H radiolabeled H12-(ADP)-liposome exhibited similar behaviors for up to 24 h after injection in normal rats,[17] indicating that the H12-(ADP)-liposomes circulate in the bloodstream without any leakage of ADP, the plasma concentration curves of ^{14}C radioactivity and ^{3}H radioactivity and pharmacokinetic parameters in thrombocytopenic rats were different. However, previous *in vivo* hemostatic studies of H12-(ADP)-liposomes clearly showed that the tail vein bleeding times for busulphan-induced thrombocytopenic rats after an infusion of H12-(ADP)-liposomes (10 mg lipids/kg) were significantly reduced compared with that of nontreatment rats.[14,16] These results indicate that the H12-(ADP)-liposomes likely circulate in the bloodstream in a form available for exerting hemostasis until they reach the site of a vascular injury, and successfully augment hematostatic effects in thrombocytopenic rats.

Tissue Distribution

Liposomes are generally captured and degraded by the mononuclear phagocyte system (MPS) in the liver and spleen, such as by Kupffer cells and splenic macrophages.[25] As expected, both the ^{14}C radioactivity and ^{3}H radioactivity of the H12-(ADP)-liposomes were mainly distributed in the liver and spleen in thrombocytopenic rats at 2, 6, and 24 h after the administration of ^{14}C, ^{3}H-labeled H12-(ADP)-liposomes at a dose of 10 mg lipids/kg (Fig. 3), but were scarcely distributed in kidney, lung, and heart (data not shown). This result is in general agreement with results reported in a previous study involving similar pharmacokinetic studies in normal rats.[17] A previous *in vivo* and *in vitro* finding reported that HbV, which has similar characteristics in terms of liposomal structure to H12-(ADP)-liposomes, was mainly distributed to the liver and spleen, and the specific uptake and degradation of HbV was observed only in macrophage cells (RAW 264.7 cells) but not in parenchymal and endothelial cells in the liver.[26] These results strongly suggest that the majority of the H12-(ADP)-liposomes are also scavenged and degraded by the MPS, likely by Kupffer cells or splenic macrophages, in thrombocytopenic rats.

As the liver and spleen are the major distribution tissues for H12-(ADP)-liposomes in both normal and thrombocytopenic rats, the hepatic and splenic distribution of H12-(ADP)-liposomes was compared. Figure 3 provides information on the tissue distribution in liver and spleen at 2, 6, and 24 h after the administration of ^{14}C, ^{3}H-labeled H12-(ADP)-liposomes at a dose of 10 mg lipids/kg to normal and thrombocytopenic rats. The hepatic distributions of both ^{14}C radioactivity and ^{3}H radioactivity in thrombocytopenic rats were higher than that in normal rats (Figs. 3a and 3b). In a previous study, Telgenhoff et al.[27] reported that the greatest number of activated macrophages in the liver were observed in rats treated with the anticancer drug, cisplatin, as evidenced by light and electron microscopic analyses. In addition, the disease conditions including thrombocytopenia that induced cytokines productions may enhance the phagocyte activity of macrophages. Therefore, the possibilities that either/both busulphan or/and disease conditions such as thrombocytopenia may influence to the phagocyte activity of Kupffer cells and other type of macrophages (splenic macrophages and bone marrow macrophages etc.) leading to a change in the tissue distribution of H12-(ADP)-liposomes in busulphan-induced thrombocytopenic rats cannot be excluded. Further study will be necessary to elucidate whether the treatment with anticancer drugs or thrombocytopenic condition influence the macrophage activity from the viewpoint of future clinical applications of H12-(ADP)-liposomes in patients with anticancer drugs induced thrombocytopenia. On the contrary, the distribution of both ^{14}C radioactivity and ^{3}H radioactivity in the spleen was decreased in thrombocytopenic rats compared with that in normal rats (Figs. 3c and 3d). In addition, no difference was found in the tissue distribution of both the ^{14}C radioactivity and ^{3}H radioactivity of the H12-(ADP)-liposomes in other organs (kidney, lung, and heart) between normal and thrombocytopenia rats (data not shown). These data indicate that the H12-(ADP)-liposomes are mainly distributed to the liver and spleen in thrombocytopenic rats, and that the tissue distribution in the liver and spleen was changed when thrombocytopenia was present.

To develop an H12-(ADP)-liposome preparation for use as a platelet alternative, it is important to have an extensive knowledge of the characteristics of the biodegradable properties of

DOI 10.1002/JPS.23692

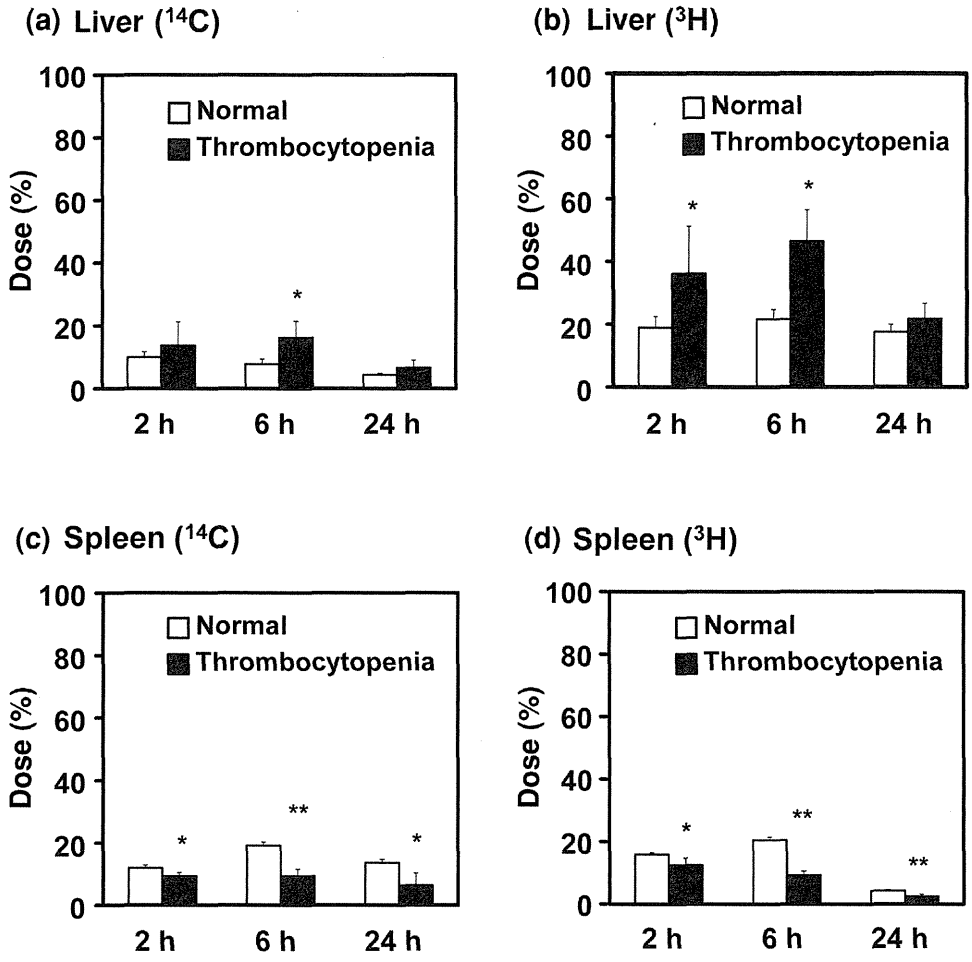

Figure 3. The hepatic distribution of (a) ^{14}C radioactivity and (b) 3H radioactivity and splenic distribution of (c) ^{14}C radioactivity and (d) 3H radioactivity at 2, 6, and 24 h after an intravenous injection of 3H, ^{14}C radiolabled H12-(ADP)-liposome at a dose of 10 mg lipids/kg to normal rats (open bar) and thrombocytopenic rats (closed bar). The data for the normal rats were cited from our previously reported paper.[17] Each bar represents the mean ± SD ($n = 4$). $^{*}p < 0.05$, $^{**}p < 0.01$ versus normal rats.

the compound (no accumulation or retention in tissues). In the present study, both the ^{14}C radioactivity and ^{3}H radioactivity of the H12-(ADP)-liposomes were eliminated from the bloodstream and organs, and the activity essentially disappeared within 7 days after injection of the H12-(ADP)-liposomes (data not shown), indicating that H12-(ADP)-liposomes and components derived from them do not accumulate in the body to any extent. Therefore, H12-(ADP)-liposomes contain the appropriate components and have the potential for use as a synthetic platelet substitute, because they possess acceptable biodegradable properties, even under conditions of thrombocytopenia.

Excretion

In order to identify the excretion pathway of the H12-(ADP)-liposomes in thrombocytopenic rats, the levels of ^{14}C and ^{3}H in urine and feces were measured (Fig. 4). The ^{14}C was excreted mainly in the urine (Fig. 4a; 85.7 ± 3.6% of the injected dose at 5 days after injection), but the levels were low in feces (Fig. 4c; 14.5 ± 6.9% of the injected dose at 5 day after injection). We previously showed that most of the encapsulated ADP in the H12-(ADP)-liposomes was mainly metabolized to allantoin, which is the final metabolite of ADP in rodents,[28] and was excreted into the urine within 7 days after the injection in normal rats.[17] Therefore, the ADP encapsulated within H12-liposomes was completely metabolized and excreted into the urine, even though ADP was encapsulated within the liposome, in thrombocytopenic rats. Furthermore, the enhanced excretion of ^{14}C of ADP in feces was observed in thrombocytopenic rats as compared with normal rats (Fig. 4c). Although it is difficult to explain these unexpected results, these phenomena suggested that a part of encapsulated ADP and its metabolites in H12-(ADP)-liposomes are eliminated by bile excretion pathway, and it increases in thrombocytopenia. To clarify whether it is specific to busulphan, it will be necessary to examine the same experiments under the similar thrombocytopenia conditions induced by other anticancer agents.

On the contrary, the majority of the ^{3}H was excreted in the feces (Fig. 4d; 70.8 ± 7.9% of the injected dose at 5 days after injection), and excretion into the urine was essentially nil (Fig. 4b). This result is in agreement with the disposition of H12-(ADP)-liposome in normal rats[17] and HbV that uses an HbV-labeled outer membrane with [^{3}H] cholesterol.[26] A previous report showed that cholesterol in liposomes reappears in the blood mainly as lipoprotein–cholesterol complexes after entrapment in Kupffer cells and should then be excreted via the bile after entrapment of the lipoprotein cholesterol com-

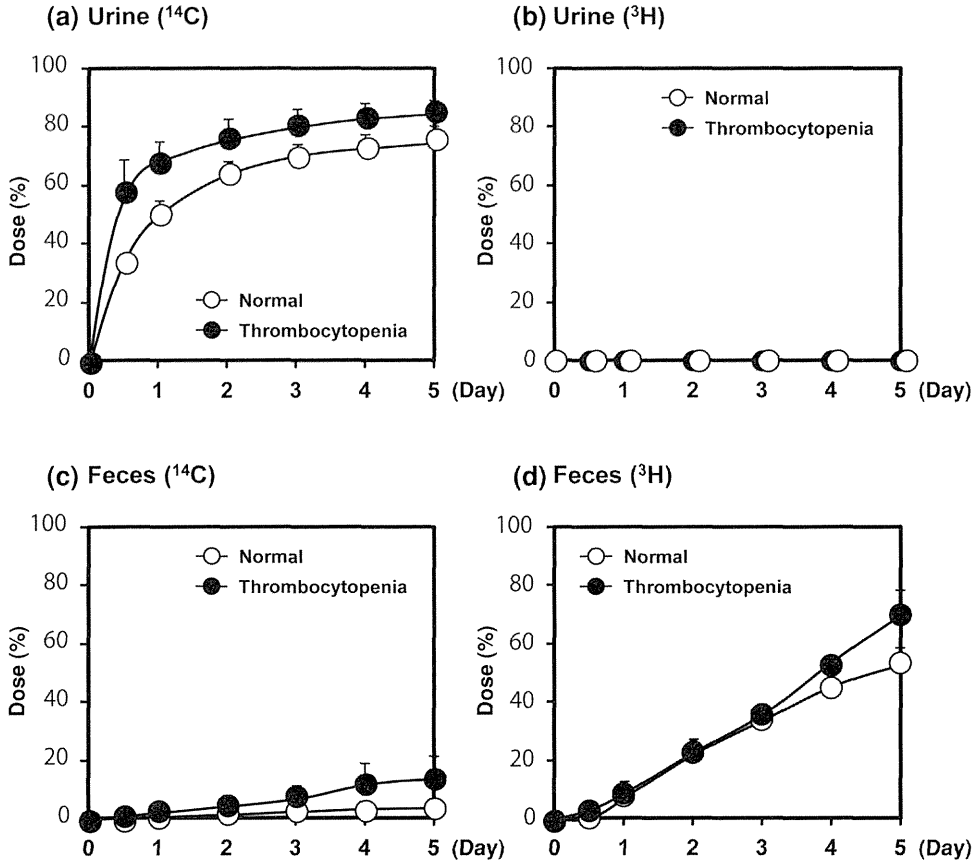

Figure 4. Time course for radioactivity in urine and feces after the administration of ^{3}H, ^{14}C radiolabled H12-(ADP)-liposome at a dose of 10 mg lipids/kg to normal rats (open circle) and thrombocytopenic rats (closed circle). The data for the normal rats were cited from our previously reported paper.[17] Each point represents the mean ± SD (n = 4).

plex by hepatocytes.[29] Therefore, under conditions of thrombocytopenia, it is possible that the cholesterol in the H12-(ADP)-liposome is metabolized and excreted in the same manner as the other liposome components, as reported by Kuipers et al.[29] In fact, the amount of fecal excretion of ^{3}H at 5 days after injection in thrombocytopenic rats was higher than that in normal rats (Fig. 4d) with the increment of hepatic distribution (Fig. 3b).

These results indicate that, even though the H12-(ADP)-liposomes and its components retained their desirable excretion properties in thrombocytopenic rats, the excretion pathway of the H12-(ADP)-liposomes components in thrombocytopenic rats were the same as that in normal rats.

CONCLUSIONS

Our objective was to develop H12-(ADP)-liposome that possess the characteristics of, not only better pharmacological effects (suitable blood retention), but also acceptable biodegradable properties (no retention in the body), and to document these characteristics in, not only normal, but also under conditions of thrombocytopenia. In the present study, we provide the first demonstration of the preparation and function of H12-(ADP)-liposomes and show that that the disposition of H12-(ADP)-liposomes and components derived from them in thrombocytopenic rats induced by busulphan are as follows. After the systemic circulation of the H12-(ADP)-liposomes in the blood stream, they were mainly distributed to the liver and spleen, where they are degraded by the MPS. Finally, the encapsulated ADP and membrane component (cholesterol) are eliminated mainly to the urine and feces, respectively. This successive disposition of H12-(ADP)-liposomes in thrombocytopenic conditions was the same as that in normal rats. However, the amount of urinary and fecal excretion of H12-(ADP)-liposomes and components derived from them after injection in thrombocytopenic rats were higher than that in normal rats with a decrease in blood retention and increment of hepatic distribution. As the thrombocytopenic rats used in this study reflect the clinical features of patients with thrombocytopenia induced by anticancer drugs, a similar phenomenon would be expected in clinical situations. The above findings provide useful information, such as dosing regimens, for the development of the H12-(ADP)-liposomes for use as a platelet substitute in future clinical applications.

ACKNOWLEDGMENTS

We would like to thank Shunsuke Katsuno and Manami Arai at Waseda University for preparation of liposome samples. We also thank Mai Hashimoto at Kumamoto University for technical assistance in the present study. This work was supported in part by Health and Labor Sciences Research Grants (Research on Public Essential Drugs and Medical Devices) from the Ministry of Health, Labour and Welfare, Japan.

DOI 10.1002/JPS.23692

REFERENCES

1. Blajchman MA. 2003. Substitutes and alternatives to platelet transfusions in thrombocytopenic patients. J Thromb Haemost 1(7):1637–1641.

2. Rybak ME, Renzulli LA. 1993. A liposome based platelet substitute, the plateletsome, with hemostatic efficacy. Biomater Artif Cells Immobilization Biotechnol 21(2):101–118.

3. Graham SS, Gonchoroff NJ, Miller JL. 2001. Infusible platelet membranes retain partial functionality of the platelet GPIb/IX/V receptor complex. Am J Clin Pathol 115(1):144–147.

4. Levi M, Friederich PW, Middleton S, de Groot PG, Wu YP, Harris R, Biemond BJ, Heijnen HF, Levin J, ten Cate JW. 1999. Fibrinogen-coated albumin microcapsules reduce bleeding in severely thrombocytopenic rabbits. Nat Med 5(1):107–111.

5. Agam G, Livne AA. 1992. Erythrocytes with covalently bound fibrinogen as a cellular replacement for the treatment of thrombocytopenia. Eur J Clin Invest 22(2):105–112.

6. Casals E, Verdaguer A, Tonda R, Galan A, Escolar G, Estelrich J. 2003. Atomic force microscopy of liposomes bearing fibrinogen. Bioconjug Chem 14(3):593–600.

7. Coller BS, Springer KT, Beer JH, Mohandas N, Scudder LE, Norton KJ, West SM. 1992. Thromboerythrocytes. In vitro studies of a potential autologous, semi-artificial alternative to platelet transfusions. J Clin Invest 89(2):546–555.

8. Takeoka S, Teramura Y, Okamura Y, Handa M, Ikeda Y, Tsuchida E. 2001. Fibrinogen-conjugated albumin polymers and their interaction with platelets under flow conditions. Biomacromolecules 2(4):1192–1197.

9. Suzuki H, Okamura Y, Ikeda Y, Takeoka S, Handa M. 2011. Ultrastructural analysis of thrombin-induced interaction between human platelets and liposomes carrying fibrinogen gamma-chain dodecapeptide as a synthetic platelet substitute. Thromb Res 128(6):552–559.

10. Tokutomi K, Tagawa T, Korenaga M, Chiba M, Asai T, Watanabe N, Takeoka S, Handa M, Ikeda Y, Oku N. 2011. Decoration of fibrinogen gamma-chain peptide on adenosine diphosphate-encapsulated liposomes enhances binding of the liposomes to activated platelets. Int J Pharm 407(1–2):151–157.

11. Tokutomi K, Tagawa T, Korenaga M, Chiba M, Asai T, Watanabe N, Takeoka S, Handa M, Ikeda Y, Oku N. 2012. Ability of fibrinogen gamma-derived dodecapeptides with different sequences to bind to rat platelets. Int J Pharm 438(1–2):296–301.

12. Nishikawa K, Hagisawa K, Kinoshita M, Shono S, Katsuno S, Doi M, Yanagawa R, Suzuki H, Iwaya K, Saitoh D, Sakamoto T, Seki S, Takeoka S, Handa M. 2012. Fibrinogen gamma-chain peptide-coated, ADP-encapsulated liposomes rescue thrombocytopenic rabbits from non-compressible liver hemorrhage. J Thromb Haemost 10(10):2137–2148.

13. Okamura Y, Eto K, Maruyama H, Handa M, Ikeda Y, Takeoka S. 2010. Visualization of liposomes carrying fibrinogen gamma-chain dodecapeptide accumulated to sites of vascular injury using computed tomography. Nanomedicine 6(2):391–396.

14. Okamura Y, Katsuno S, Suzuki H, Maruyama H, Handa M, Ikeda Y, Takeoka S. 2010. Release abilities of adenosine diphosphate from phospholipid vesicles with different membrane properties and their hemostatic effects as a platelet substitute. J Control Release 148(3):373–379.

15. Okamura Y, Maekawa I, Teramura Y, Maruyama H, Handa M, Ikeda Y, Takeoka S. 2005. Hemostatic effects of phospholipid vesicles carrying fibrinogen gamma chain dodecapeptide in vitro and in vivo. Bioconjug Chem 16(6):1589–1596.

16. Okamura Y, Takeoka S, Eto K, Maekawa I, Fujie T, Maruyama H, Ikeda Y, Handa M. 2009. Development of fibrinogen gamma-chain peptide-coated, adenosine diphosphate-encapsulated liposomes as a synthetic platelet substitute. J Thromb Haemost 7(3):470–477.

17. Taguchi K, Ujihira H, Ogaki S, Watanabe H, Fujiyama A, Doi M, Okamura Y, Takeoka S, Ikeda Y, Handa M, Otagiri M, Maruyama T. 2013. Pharmacokinetic study of the structural components of adenosine diphosphate-encapsulated liposomes coated with fibrinogen gamma-chain dodecapeptide as a synthetic platelet substitute. Drug Metab Dispos 41:1584–1591.

18. Walsh TJ, Yeldandi V, McEvoy M, Gonzalez C, Chanock S, Freifeld A, Seibel NI, Whitcomb PO, Jarosinski P, Boswell G, Bekersky I, Alak A, Buell D, Barret J, Wilson W. 1998. Safety, tolerance, and pharmacokinetics of a small unilamellar liposomal formulation of amphotericin B (AmBisome) in neutropenic patients. Antimicrob Agents Chemother 42(9):2391–2398.

19. Bekersky I, Fielding RM, Dressler DE, Kline S, Buell DN, Walsh TJ. 2001. Pharmacokinetics, excretion, and mass balance of ^{14}C after administration of ^{14}C-cholesterol-labeled AmBisome to healthy volunteers. J Clin Pharmacol 41(9):963–971.

20. Taguchi K, Maruyama T, Iwao Y, Sakai H, Kobayashi K, Horinouchi H, Tsuchida E, Kai T, Otagiri M. 2009. Pharmacokinetics of single and repeated injection of hemoglobin-vesicles in hemorrhagic shock rat model. J Control Release 136(3):232–239.

21. Frank R, Hargreaves R. 2003. Clinical biomarkers in drug discovery and development. Nat Rev Drug Dis 2(7):566–580.

22. Yang C, Li YC, Kuter DJ. 1999. The physiological response of thrombopoietin (c-Mpl ligand) to thrombocytopenia in the rat. Br J Haematol 105(2):478–485.

23. Yamakawa N, Suemasu S, Watanabe H, Tahara K, Tanaka K, Okamoto Y, Ohtsuka M, Maruyama T, Mizushima T. 2013. Comparison of pharmacokinetics between loxoprofen and its derivative with lower ulcerogenic activity, fluoro-loxoprofen. Drug Metab Pharmacokinet 28(2):118–124.

24. Taguchi K, Miyasato M, Watanabe H, Sakai H, Tsuchida E, Horinouchi H, Kobayashi K, Maruyama T, Otagiri M. 2011. Alteration in the pharmacokinetics of hemoglobin-vesicles in a rat model of chronic liver cirrhosis is associated with Kupffer cell phagocyte activity. J Pharm Sci 100(2):775–783.

25. Kiwada H, Matsuo H, Harashima H. 1998. Identification of proteins mediating clearance of liposomes using a liver perfusion system. Adv Drug Deliv Rev 32(1–2):61–79.

26. Taguchi K, Urata Y, Anraku M, Maruyama T, Watanabe H, Sakai H, Horinouchi H, Kobayashi K, Tsuchida E, Kai T, Otagiri M. 2009. Pharmacokinetic study of enclosed hemoglobin and outer lipid component after the administration of hemoglobin vesicles as an artificial oxygen carrier. Drug Metab Dispos 37(7):1456–1463.

27. Telgenhoff DJ, Aggarwal SK, Johnson BN. 1999. Histochemical and morphological identification of Kupffer cells activated by cisplatin. Anticancer Res 19(2A):1005–1010.

28. Coulson R. 1976. Metabolism and excretion of exogenous adenosine 3':5'-monophosphate and guanosine 3':5'-monophosphate. Studies in the isolated perfused rat kidney and in the intact rat. J Biol Chem 251(16):4958–4967.

29. Kuipers F, Spanjer HH, Havinga R, Scherphof GL, Vonk RJ. 1986. Lipoproteins and liposomes as in vivo cholesterol vehicles in the rat: Preferential use of cholesterol carried by small unilamellar liposomes for the formation of muricholic acids. Biochim Biophys Acta 876(3):559–566.

1521-009X/41/8/1584–1591$25.00
DRUG METABOLISM AND DISPOSITION
http://dx.doi.org/10.1124/dmd.112.050005
Drug Metab Dispos 41:1584–1591, August 2013

Pharmacokinetic Study of the Structural Components of Adenosine Diphosphate-Encapsulated Liposomes Coated with Fibrinogen γ-Chain Dodecapeptide as a Synthetic Platelet Substitute[S]

Kazuaki Taguchi, Hayato Ujihira, Shigeru Ogaki, Hiroshi Watanabe, Atsushi Fujiyama, Mami Doi, Yosuke Okamura, Shinji Takeoka, Yasuo Ikeda, Makoto Handa, Masaki Otagiri, and Toru Maruyama

Department of Biopharmaceutics, Graduate School of Pharmaceutical Sciences (K.T., H.U., S.O., H.W., M.O., T.M.), and Center for Clinical Pharmaceutical Sciences (H.W., T.M.), Kumamoto University, Kumamoto, Japan; Department of Life Science and Medical Bioscience, Graduate School of Advanced Science and Engineering, Waseda University, Tokyo, Japan (A.F., M.D., S.T., Y.I); Institute of Innovative Science and Technology, Tokai University, Tokyo, Japan (Y.O.); Department of Transfusion Medicine & Cell Therapy, Keio University, Tokyo, Japan (M.H.); and Faculty of Pharmaceutical Sciences and DDS Research Institute, Sojo University, Kumamoto, Japan (M.O.)

Received November 8, 2012; accepted June 4, 2013

ABSTRACT

Fibrinogen γ-chain (dodecapeptide HHLGGAKQAGDV, H12)–coated, ADP-encapsulated liposomes [H12-(ADP)-liposomes] were developed as a synthetic platelet alternative that specifically accumulates at bleeding sites as the result of interactions with activated platelets via glycoprotein IIb/IIIa and augments platelet aggregation by releasing ADP. The aim of this study is to characterize the pharmacokinetic properties of H12-(ADP)-liposomes and structural components in rats, and to predict the blood retention of H12-(ADP)-liposomes in humans. With use of H12-(ADP)-liposomes in which the encapsulated ADP and liposomal membrane cholesterol were radiolabeled with ^{14}C and ^{3}H, respectively, it was found that the time courses for the plasma concentration curves of ^{14}C and ^{3}H radioactivity showed that the H12-(ADP)-liposomes remained intact in the blood circulation for up to 24 hours after injection, and were mainly distributed to the liver and spleen. However, the ^{14}C and ^{3}H radioactivity of H12-(ADP)-liposomes disappeared from organs within 7 days after injection. The encapsulated ADP was metabolized to allantoin, which is the final metabolite of ADP in rodents, and was mainly eliminated in the urine, whereas the cholesterol was mainly eliminated in feces. In addition, the half-life of the H12-(ADP)-liposomes in humans was predicted to be approximately 96 hours from pharmacokinetic data obtained for mice, rats, and rabbits using an allometric equation. These results suggest that the H12-(ADP)-liposome has potential with proper pharmacokinetic and acceptable biodegradable properties as a synthetic platelet substitute.

Introduction

As the numbers of patients with hematologic malignancies and solid tumors increase, platelet transfusion represents one of the most essential prophylactic or therapeutic treatments, because these disorders induce severe thrombocytopenia caused by the intensive chemotherapy, surgical procedures, and radiotherapy. However, platelet transfusion can introduce a variety of complications such as bacterial infection, allergic reaction, and acute lung injury. In addition, donated platelet for blood transfusions can only be stored for a period of 4 days in Japan and 5–7 days in the United States and Europe. This has become a serious concern in our aging society and a stable supply in an emergency situation such as disasters and pandemics needs to be on hand. To solve these problems, various platelet substitutes, which consist of materials derived from blood components, have been developed (Blajchman, 2003), such as solubilized platelet membrane protein conjugated liposomes (plateletsome) (Rybak and Renzulli, 1993), infusible platelet membranes (Graham et al., 2001), fibrinogen-coated albumin microcapsules (synthocyte) (Levi et al., 1999), red blood cells with bound fibrinogen (Agam and Livne, 1992), liposomes bearing fibrinogen (Casals et al., 2003), arginine-glycine-aspartic acid (RGD) peptide-bound red blood cells (thromboerythrocyte) (Coller et al., 1992), and fibrinogen-conjugated albumin polymers (Takeoka et al., 2001). However, these platelet substitutes have not yet been approved for clinical use.

ADP-encapsulated liposomes modified with a dodecapeptide (HHLGGAKQAGDV, H12) [H12-(ADP)-liposome] were developed as a new type of synthetic platelet alternative. The glycoprotein

This research was supported in part by the Japanese Ministry of Health, Labour, and Welfare [Health and Labor Sciences Research Grants on Research on Public Essential Drugs and Medical Devices to S.T., Y.I., M.H., and T.M.].
dx.doi.org/10.1124/dmd.112.050005.
[S]This article has supplemental material available at dmd.aspetjournals.org.

ABBREVIATIONS: CL, clearance; DHSG, 1,5-dihexadecyl-*N*-succinyl-L-glutamate; DPPC, 1,2-dipalmitoyl-*sn*-glycero-3-phosphatidylcholine; GP, glycoprotein; H12, HHLGGAKQAGDV; H12-(ADP)-liposome, ADP-encapsulated liposomes modified with a dodecapeptide; HbV, hemoglobin vesicle; HPLC, high-performance liquid chromatography; ID, injected dose; MPS, mononuclear phagocyte system; PEG, polyethyleneglycol; PEG-DSPE, 2-distearoyl-*sn*-glycero-3-phosphatidylethanolamine-*N*-[monomethoxypoly(ethyleneglycol)]; RGD, arginine-glycine-aspartic acid; $t_{1/2}$, half-life; V_{dss}, distribution volume.

(GP) IIb/IIIa, which is present on the platelet membranes, is converted from an inactive to an active form when platelets adhere to collagen that is exposed on sites of vascular injury (Takagi et al., 2002; Xiao et al., 2004), and platelet aggregation is mediated by fibrinogen by bridging adjacent platelets through GPIIb/IIIa in an activation-dependent manner in the circulation. Among several GPIIb/IIIa recognized sequence sites in fibrinogen such as the RGD-based sequences (^{95}RGDF^{98} and ^{572}RGDS^{575} in the Aα chains) and H12 (^{400}HHLGGAKQAGDV^{411}) in the carboxy-terminus of the γ-chain (Kloczewiak et al., 1982, 1984; Hawiger et al., 1989), H12 is a specific binding site of the ligand for activated GPIIb/IIIa (Lam et al., 1987; Andrieux et al., 1989), whereas RGD-related peptides are nonspecific with respect to a wide variety of integrins from various cell types (Phillips et al., 1991). In addition, when ADP is released from activated platelets, it functions as a potent platelet agonist. Thus, these modifications to H12-(ADP)-liposomes enable them to specifically interact with activated platelets, resulting in platelet aggregation. In fact, H12-liposomes with polyethyleneglycol (PEG)-surface modification specifically accumulate at the site of an injury in vivo and were determined to shorten bleeding time in a dose-dependent manner in a thrombocytopenic rat and a rabbit model (Okamura et al., 2005, 2009, 2010a,b; Nishikawa et al., 2012). Therefore, these findings prompted us to conclude that H12-(ADP)-liposomes have considerable potential for use as an alternative for actual platelets in clinical settings.

Before new drugs are approved for clinical use, they are required to undergo a wide variety of evaluations, including physicochemical tests, preclinical studies, and clinical trials. As described above, preclinical studies of H12-(ADP)-liposomes have resulted in pharmacological evidence to indicate that they can be used as a platelet substitute (Okamura et al., 2005, 2009, 2010a,b; Nishikawa et al., 2012). However, information concerning pharmacokinetic properties is lacking, especially the disposition and retention of each component in tissues after injection. Our strategy for the development of H12-(ADP)-liposomes is based on the fact that not only better pharmacological effects but also acceptable biodegradable properties (no accumulation or retention) need to be documented. In addition, preclinical pharmacokinetic studies in various mammalian species are essential, because the results of such studies can be extrapolated to humans, allowing appropriate dosing regimens to be estimated in the case of humans.

In the present study, we report on an evaluation of the pharmacokinetic properties of the H12-(ADP)-liposomes and components thereof, from the standpoint of stability in the blood circulation and the metabolism and excretion of each component. For this purpose, we prepared H12-(ADP)-liposomes that were ^{14}C, ^{3}H double radiolabeled, in which the encapsulated ADP and membrane component (cholesterol) were labeled with ^{14}C and ^{3}H, respectively. Furthermore, we predicted some important pharmacokinetic parameters, especially retention in the blood circulation, in humans, based on data obtained in pharmacokinetic studies in mice, rats, and rabbits.

Materials and Methods

Reagents

Cholesterol and 1,2-dipalmitoyl-*sn*-glycero-3-phosphatidylcholine (DPPC) were purchased from Nippon Fine Chemical (Osaka, Japan), and 2-distearoyl-*sn*-glycero-3-phosphatidylethanolamine-*N*-[monomethoxypoly(ethyleneglycol)] (PEG-DSPE, 5.1 kDa) was from NOF (Tokyo, Japan). 1,5-Dihexadecyl-*N*-succinyl-L-glutamate (DHSG) and H12-PEG-Glu2C18, in which the fibrinogen γ-chain dodecapeptide (C-HHLGGAKQAGDV, Cys-H12) was conjugated to the end of the PEG-lipids, were synthesized as previous reported (Okamura et al., 2005). Allantoin, uric acid, hypoxanthine, xanthine, and ADP were obtained from Sigma-Aldrich (St. Louis, MO).

Preparation of ^{14}C, ^{3}H Double-Labeled H12-(ADP)-Liposomes

First, ^{14}C-labeled H12-(ADP)-liposomes were prepared under sterile conditions as previously reported, with minor modifications (Okamura et al., 2009). In brief, DPPC (1000 mg, 1.36 mmol), cholesterol (527 mg, 1.36 mmol), DHSG (189 mg, 272 μmol), PEG-DSPE (52 mg, 9.0 μmol), and H12-PEG-Glu2C18 (47 mg, 9.0 μmol) were dissolved in *t*-butyl alcohol and then freeze-dried. The resulting mixed lipids were hydrated with phosphate-buffered saline (pH 7.4) containing ADP (1 mM) and [8-^{14}C]ADP (1.85 MBq; Moravec Biochemicas Inc., La Brea, CA), and extruded through membrane filters (0.22 μm pore size, Durapore; Millipore, Tokyo, Japan). Liposomes were washed with phosphate-buffered saline by centrifugation (100,000*g*, 30 minutes, 4°C), and the remaining ADP was eliminated by sephadexG25. The diameter and ζ potential of the ^{14}C-labeled H12-(ADP)-liposomes used in this study are regulated at 250 $\pm$ 50 nm and -10 ± 0.9 mV, respectively. The 5–10% of added ADP was encapsulated in the inner space of the vesicle.

The ^{3}H labeling of ^{14}C-labeled H12-(ADP)-liposomes, to prepare ^{14}C and ^{3}H double-labeled H12-(ADP)-liposomes, was carried out according to a previous report (Taguchi et al., 2009). The ^{14}C-labeled H12-(ADP)-liposomes (1 ml) were mixed with [1,2-^{3}H(*N*)]cholesterol solution (10 μl), (PerkinElmer, Yokohama, Japan) and incubated for 12 hours at room temperature. ^{14}C, ^{3}H-labeled H12-(ADP)-liposomes were filtered through a sterile filter to remove aggregates (450 nm pore size). Before being used in pharmacokinetic experiments, all of the samples were mixed with unlabeled H12-(ADP)-liposomes. To utilize the same procedure using H12-(ADP)-liposomes and [1,2-^{3}H(*N*)]cholesterol, ^{3}H-labeled H12-(ADP)-liposomes, which did not contain [8-^{14}C]ADP, were prepared for the pharmacokinetic studies in mice and rabbits.

Animals

All animal experiments were undertaken in accordance with the guideline principle and procedure of Kumamoto University for the care and use of laboratory animals. Experiments were carried out with male ddY mice (28–30 g body weight; Japan SLC, Inc., Shizuoka, Japan), male Sprague-Dawley rats (180–210 g body weight; Kyudou Co., Kumamoto, Japan), and male New Zealand White rabbits (2.0–2.2 kg body weight; Biotek Co., Saga, Japan). All animals were maintained under conventional housing conditions, with food and water ad libitum in a temperature-controlled room with a 12-hour dark/light cycle.

Pharmacokinetic Studies

Administration and Collecting Blood and Organs in Rats. Twenty-four Sprague-Dawley rats were anesthetized with diethyl ether and received a single injection of ^{14}C, ^{3}H-labeled H12-(ADP)-liposomes [10 mg lipids/kg (n = 16), 20 mg lipids/kg (n = 4), and 40 mg lipids/kg (n = 4)]. In all rat groups, four rats were selected to undergo the plasma concentration test. Under ether anesthesia, approximately 200 μl blood samples in all administration groups were collected from tail vein at multiple time points after the injection of the ^{14}C, ^{3}H-labeled H12-(ADP)-liposomes (3, 10, and 30 minutes, and 1, 2, 3, 6, 12, 24, 48 and 168 hours) and the plasma was separated by centrifugation (3000*g*, 5 minutes). After collecting the last blood sample (168 hours), the rats were euthanized for excision of organs (kidney, liver, spleen, lung, and heart). Urine and feces were collected at fixed intervals in a metabolic cage. In addition, the four rats were sacrificed and organs were collected at 2, 6, and 24 hours after an injection of ^{14}C, ^{3}H-labeled H12-(ADP)-liposomes at a dose of 10 mg lipids/kg.

Administration and Collection of Blood and Organs in Mice and Rabbits. Twenty-eight ddY mice received a single injection of ^{3}H-labeled H12-(ADP)-liposomes (10 mg lipids/kg) in the tail vein under ether anesthesia. At each time after the injection of ^{3}H-labeled H12-(ADP)-liposomes (3 and 30 minutes, and 1, 3, 6, 12, and 24 hours), four mice were anesthetized with ether and blood was collected from the inferior vena cava, and plasma was obtained by centrifugation (3000*g*, 5 minutes).

Four New Zealand White rabbits received a single injection of ^{3}H-labeled H12-(ADP)-liposomes at a dose of 10 mg lipids/kg. The blood was collected from the auricular veins at each time after injection (3, 10, and 30 minutes, and

1, 2, 12, 24, 36, 48, and 72 hours), and plasma was obtained by centrifugation (3000*g*, 5 minutes).

Measurement of ^{14}C and ^{3}H Radioactivity. Plasma samples were solubilized in a mixture of Soluene-350 (PerkinElmer) and isopropyl alcohol (at a ratio of 1/1) for 24 h at 50°C. The organ samples were rinsed with saline, minced, and solubilized in Soluene-350 for 24 hours at 50°C. Urine and feces were also weighed and solubilized in Soluene-350. All samples were decolorized by treatment with a hydrogen peroxide solution after treatment of Soluene-350 or isopropyl alcohol. The ^{14}C, ^{3}H radioactivity was determined by liquid scintillation counting (LSC-5121; Aloka, Tokyo, Japan) with Hionic-Fluor (PerkinElmer).

Analysis of Metabolites of Encapsulated ADP. ADP metabolites in urine were determined by high-performance liquid chromatography (HPLC), as described previously (George et al., 2006). A part of the urine obtained in the pharmacokinetic study in rats was used for this analysis, and aliquots of urine samples (2.5 ml) were mixed with 200 μl 10% sulfuric acid. Just before the analysis, the urine samples were centrifuged and filtered through a Dismic-25cs (0.2 μm pore size; ADVANTEC, Tokyo, Japan) and diluted 10-fold with water after adjusting the pH to 7 with 0.01 N sodium hydroxide and 0.01 N sulfuric acid. A standard solution containing ADP, allantoin, uric acid, hypoxanthine, and xanthine was prepared as reported in a previous study (George et al., 2006). The HPLC system consisted of a Waters 2695 pump (Waters, Milford, MA), a Waters 2487 detector (Waters) operated at 220 nm. LC analyses were achieved with a 250 × 4 mm, 5 μm LiChrospher 100 RP-18 end-capped column (LiChroCART 250-4; Merck, Darmstadt, Germany). Furthermore, each ADP metabolite separated by HPLC was collected by a fraction collector (CHF121SA; ADVANTEC) and ^{14}C radioactivity was determined by liquid scintillation counting with Hionic-Fluor.

Interspecies Scaling of Pharmacokinetic Parameters

Allometric relationships between various pharmacokinetic parameters (P) and body weight (W) were plotted on a log-log scale. Linear regression of the logarithmic values was calculated using the least-squares method using Eq. 1 (Boxenbaum, 1984).

$$P = \alpha \cdot W^{\beta} \quad (1)$$

P is the parameter of interest [distribution volume (V_{dss}) or clearance (CL)], W is the body weight (kg), and α and β are the coefficient and exponent of the allometric equation, respectively. The average body weights of 0.034 kg (mouse), 0.242 kg (rat), 2.08 kg (rabbit), and 70 kg (human) were used for prediction of V_{dss} and CL for human. After predicting of V_{dss} and CL for humans (70 kg) using Eq. 1, the half-life for human was estimated.

Data Analysis

A noncompartmental model was used for the pharmacokinetic analysis. Each parameter, including half-life ($t_{1/2}$, h), mean residence time (h), area under the concentration-time curve (h · % of dose/ml), CL (ml/h), and V_{dss} (ml), was calculated using the moment analysis program available in Microsoft Excel (Microsoft Corporation, Redmond, WA) (Yamakawa et al., 2013). Data are shown as means ± S.D. for the indicated number of animals.

Results

Pharmacokinetics of H12-(ADP)-Liposome Components in Rats. To investigate the pharmacokinetics of each component of the H12-(ADP)-liposomes, ^{14}C, ^{3}H-labeled H12-(ADP)-liposomes, in which the encapsulated ADP was labeled with ^{14}C and the membrane component (cholesterol) was labeled with ^{3}H, were prepared (Fig. 1A). As shown in Fig. 1B and Table 1, the plasma concentration curves and pharmacokinetic parameters for ^{14}C radioactivity and ^{3}H radioactivity were similar. These data indicate that the structure of the H12-(ADP)-liposomes remained intact in the blood circulation for periods of up to 24 hours after injection in rats.

Moreover, we evaluated the tissue distribution of both the encapsulated ADP and membrane component (cholesterol) of the H12-(ADP)-liposomes. Figure 2 shows the tissue distribution in organs at 2, 6, and 24 hours after the administration of ^{14}C, ^{3}H-labeled H12-(ADP)-liposomes at a dose of 10 mg lipids/kg to rats. Among these organs, the majority of both the ^{14}C and ^{3}H radioactivity of the H12-(ADP)-liposomes were distributed in the liver and spleen. However, both the ^{14}C and ^{3}H radioactivity of the H12-(ADP)-liposomes were eliminated from each organ, and the activity essentially disappeared within 7 days after injection (unpublished data). These data indicate that the H12-(ADP)-liposomes are mainly distributed to the liver and spleen, but the retention in these organs is negligible.

To identify the excretion pathway of the H12-(ADP)-liposomes, the levels of ^{14}C and ^{3}H in urine and feces were measured (Fig. 3, A and B). The ^{14}C was excreted mainly in the urine [80.4% ± 4.9% of the injected dose (ID) at 7 days after injection], but was low in feces (7.6% ± 2.7% of ID at 7 day after injection). On the other hand, the majority of the ^{3}H was excreted in the feces (74.2% ± 5.7% of ID at 7 days after injection), and excretion into the urine was essentially nil. In addition, as shown in Fig. 3C, it is well known that, in rodents, endogenous ADP is ultimately metabolized to allantoin and excreted. Thus, we qualitatively determined the fate of the encapsulated ADP of the H12-(ADP)-liposomes using an HPLC method. Figure 3D shows the separated peaks for ADP and its metabolites in the standard solution and in a urine sample 6 hours after the administration of the H12-(ADP)-liposomes to a rat. Furthermore, to exclude the effect of endogenous ADP and its metabolites, we measured the ^{14}C radioactivity of each peak that had been separated by HPLC. As a result, almost all of the ^{14}C radioactivity was detected in the peak corresponding to allantoin, which is the final metabolite of ADP in rodents, in the urine sample (Table 2).

These results indicate that more than 75% of each structural component of the H12-(ADP)-liposome is excreted from the body within 7 days after injection, and the encapsulated ADP and membrane component (cholesterol) derived from H12-(ADP)-liposomes were metabolized to final metabolites and excreted into the urine and feces, respectively.

Dose-Dependence of H12-(ADP)-Liposomes Pharmacokinetics. Figure 4 shows the time courses for the plasma concentration for the ^{14}C, ^{3}H-labeled H12-(ADP)-liposomes administered to rats at doses of 10, 20, and 40 mg lipids/kg. No significant difference was found in the plasma concentration curve or pharmacokinetic parameters among all groups (Fig. 4, A and B). In fact, a linear relationship between the administration dose and the area under the concentration-time curve was found, the values for which were calculated based on the lipids concentration (Fig. 4C). These data indicate that the disposition of the H12-(ADP)-liposomes is linear for a dose of 40 mg lipids/kg.

Moreover, the tissue distribution of both the encapsulated ADP and the membrane lipids component (cholesterol) of the ^{14}C, ^{3}H-labeled H12-(ADP)-liposomes was evaluated at 7 days after the injection of H12-(ADP)-liposomes at doses of 10, 20, 40 mg lipids/kg. The level of ^{14}C and ^{3}H radioactivity was nearly undetectable in the observed organs (kidney, liver, spleen, lung, and heart) (unpublished data). In addition, the radioactive ^{14}C was excreted mainly in the urine (80.4% ± 4.9%, 52.1% ± 3.6%, and 58.4% ± 7.1% of ID at 7 days after the injection at doses of 10, 20, and 40 mg lipids/kg, respectively), but was low in feces (7.6% ± 2.7%, 6.5% ± 2.9%, and 2.5% ± 1.9% of ID at 7 days after the injection at doses of 10, 20, and 40 mg lipids/kg, respectively). On the other hand, the majority of the radioactive ^{3}H was excreted in the feces (74.2% ± 5.7%, 98.9% ± 14.9%, and 70.6% ± 6.2% of ID at 7 days after the injection at doses of 10, 20, and 40 mg lipids/kg, respectively), and a small portion of the ^{3}H radioactivity was

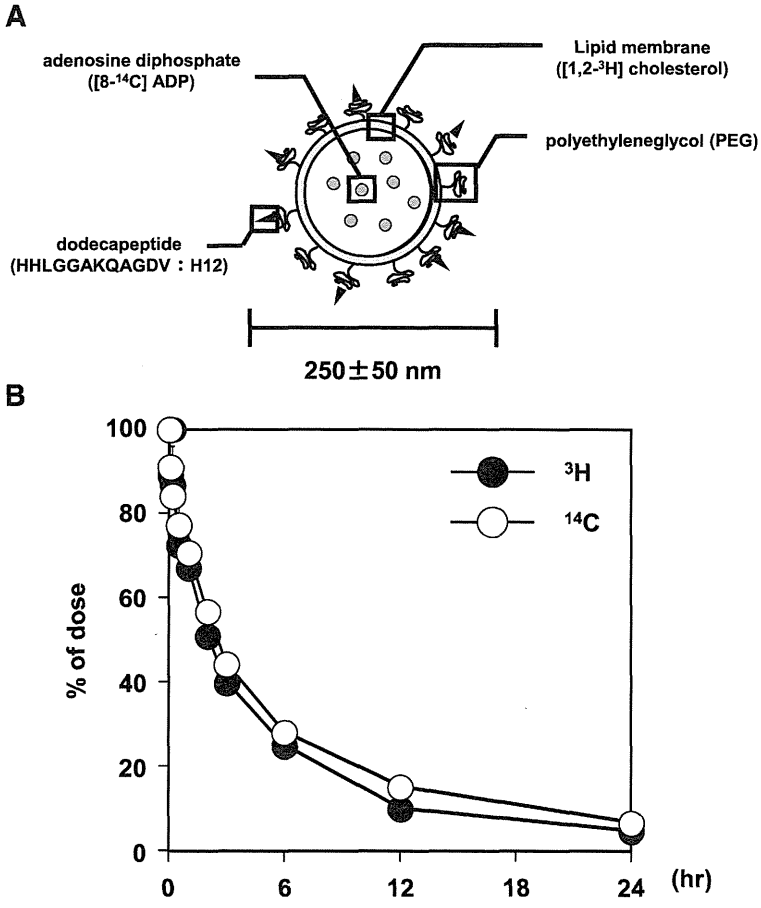

Fig. 1. (A) Structure and regiospecifically ^{3}H- and ^{14}C-radiolabeled H12-(ADP)-liposome. (B) Time course for the plasma concentration of ^{3}H and ^{14}C radiolabeled H12-(ADP)-liposome after intravenous injection at a dose of 10 mg lipids/kg to rats. Each point represents the mean ± S.D. (n = 4).

excreted into the urine. These data indicate that more than 75% of H12-(ADP)-liposomes are eliminated within 7 days after injection and retention in the body can be limited to detect at a dose of up to 40 mg lipids/kg.

Pharmacokinetics of the H12-(ADP)-Liposomes in Mice and Rabbits. To calculate the pharmacokinetic parameters of the H12-(ADP)-liposomes in mice and rabbits, the ^{3}H-labeled H12-(ADP)-liposomes were administered to mice and rabbits at a dose of 10 mg lipids/kg. According to the pharmacokinetic parameters calculated from the plasma concentration curve, the CL and V_{dss} of the ^{3}H-labeled H12-(ADP)-liposomes in mice were 0.54 ± 0.12 ml/h and 3.81 ± 0.35 ml, respectively, whereas the values in the case of rabbits were 23.5 ± 2.8 ml/h and 827 ± 163 ml, respectively (Supplemental Table 1).

Prediction of Pharmacokinetics of the H12-(ADP)-Liposomes in Humans. To predict the pharmacokinetics in humans, we examined the allometric relationship between V_{dss} and body weight (Fig. 5A) and CL and body weight (Fig. 5B) in mice, rats, and rabbits using the results summarized in Table 1 and Supplemental Table 1. As shown in Fig. 5, a good correlation in both relationships was observed. Furthermore, we calculated the half-life, based on extrapolation, of the H12-(ADP)-liposomes that were administered at a dose of 10 mg lipids/kg in humans to be approximately 96 hours.

TABLE 1

The pharmacokinetic parameters of inner ADP ([8-^{14}C]ADP) and outer lipid membranes ([1,2-$^{3}H(N)$]cholesterol) derived from ^{3}H- and ^{14}C-radiolabeled H12-(ADP)-liposomes after an intravenous injection at doses of 10, 20, and 40 mg lipids/kg to rats

Each value represents the mean ± S.D. (n = 4).

Parameter	10 mg lipid/kg		20 mg lipid/kg		40 mg lipid/kg	
	^{3}H	^{14}C	^{3}H	^{14}C	^{3}H	^{14}C
$t_{1/2}$ (h)	8.18 ± 0.77	8.21 ± 1.01	7.48 ± 0.56	7.63 ± 0.82	6.34 ± 0.53	7.94 ± 1.10
MRT (h)	10.2 ± 1.18	10.4 ± 1.46	9.20 ± 0.51	10.1 ± 1.00	7.65 ± 0.27	10.7 ± 0.97
AUC (h · % of dose/ml)	58.4 ± 6.45	54.2 ± 10.1	54.0 ± 1.97	67.8 ± 3.86	56.0 ± 1.94	84.4 ± 5.68
CL (ml/h)	1.73 ± 0.18	1.89 ± 0.32	1.85 ± 0.07	1.48 ± 0.08	1.79 ± 0.06	1.19 ± 0.07
V_{dss} (ml)	17.7 ± 3.49	19.5 ± 3.61	17.0 ± 0.58	14.8 ± 0.64	13.7 ± 0.58	12.6 ± 0.98

AUC, area under the concentration-time curve; MRT, mean residence time.

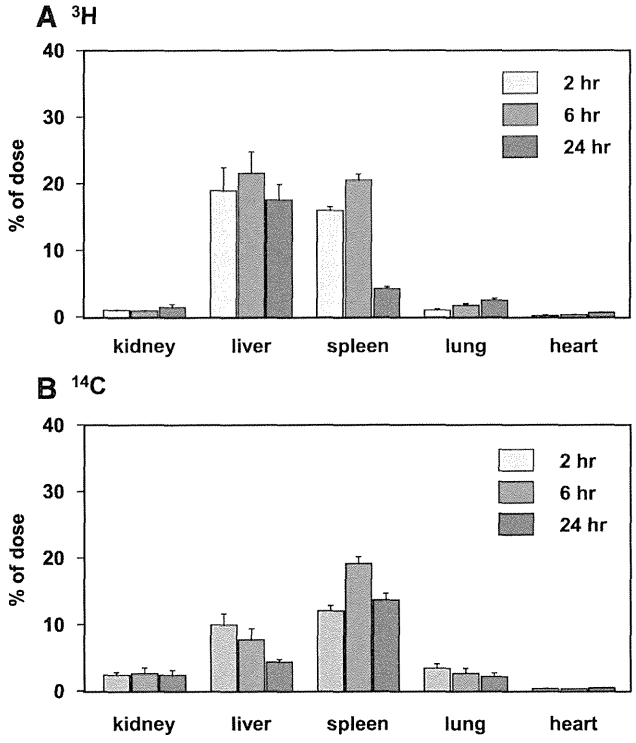

Fig. 2. The tissue distribution of ^{3}H (A) and ^{14}C radioactivity (B) at 2, 6, and 24 hours after an intravenous injection of ^{3}H- and ^{14}C-radiolabeled H12-(ADP)-liposome at a dose of 10 mg lipids/kg to rats. Each point represents the mean ± S.D. (n = 4).

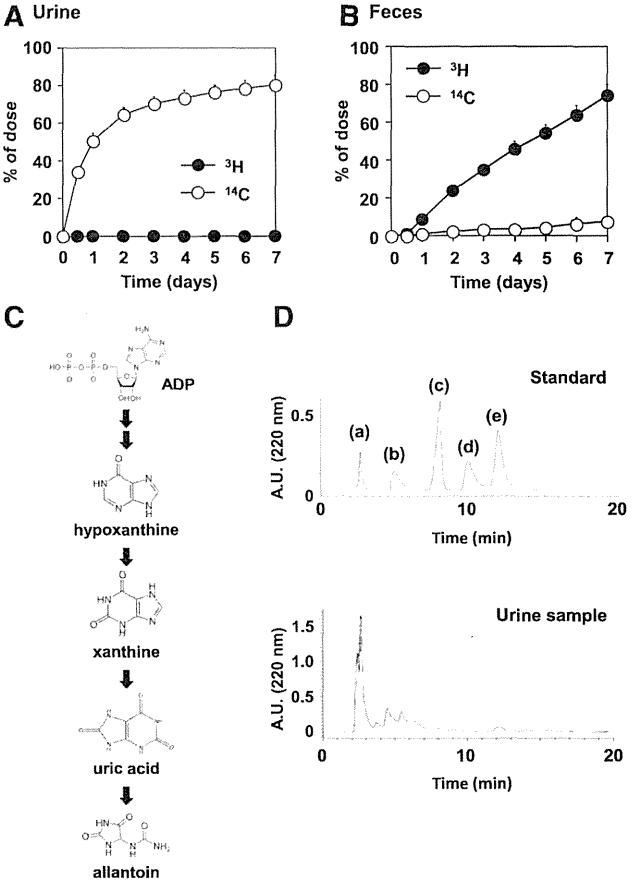

Fig. 3. Time course for radioactivity in urine (A) and feces (B) after the administration of ^{3}H- and ^{14}C-radiolabeled H12-(ADP)-liposome to rats. Each point represents the mean ± S.D. (n = 4). (C) Scheme of metabolism pathway from ADP to allantoin in rodents. (D) Chromatogram of standard mixture and urine sample analyzed by HPLC. The standard peaks are (a) allantoin, (b) ADP, (c) uric acid, (d) hypoxanthine, and (e) xanthine. The urine sample was collected 6 hours after intravenous injection of ^{3}H- and ^{14}C-radiolabeled H12-(ADP)-liposome at a dose of 10 mg lipids/kg to rats.

Discussion

In the present study, the pharmacokinetic properties of H12-(ADP)-liposomes and structural components thereof, including the encapsulated ADP and membrane components (cholesterol), were characterized. The findings confirmed that the product has proper pharmacological functions and acceptable biodegradable properties (little retention). This leads to the conclusion that the H12-(ADP)-liposomes have the potential for use as a synthetic platelet substitute from the viewpoint of the pharmacokinetic properties in rodents.

We encapsulated ADP into H12 coated liposomes to strengthen the hemostatic ability of the H12 coated liposome as a platelet substitute, because this physiologically relevant platelet agonist is stored in dense granules and released upon cellular activation, and then functions to reinforce or maintain platelet aggregation through corresponding platelet nucleotide receptors P2Y1 and P2Y12. Thus, the stable encapsulation of ADP in liposomes permits them to function at sites of vascular injuries. The findings herein clearly show that, for up to 24 hours after injection in rats, the plasma concentration curves for ^{14}C-, ^{3}H-radiolabeled H12-(ADP)-liposome exhibited similar behaviors (Fig. 1), indicating that the H12-(ADP)-liposomes circulate in the bloodstream without any leakage of ADP. In addition, we also realized that the nonliposomal ADP was immediately eliminated from blood (unpublished data), because ADP released into blood was metabolized by leukocytes, erythrocytes, and endothelial cells (Marcus et al., 2003; Heptinstall et al., 2005). This means that ADP encapsulated in the vesicle has advantages that are not only specific delivery ADP to injury site but also improvement of the blood retention of ADP. Previous in vivo hemostatic studies of H12-(ADP)-liposomes using a rat model with busulphan-induced thrombocytopenia (platelet counts; $1.9 \pm 0.2 \times 10^{5}\ \mu l^{-1}$) clearly showed that the tail vein bleeding times of thrombocytopenic rats after an infusion of H12-(ADP)-liposomes (10 mg lipids/kg) were significantly reduced compared with that of controls [H12-liposome (10 mg lipids/kg) and (ADP)-liposome (10 mg lipids/kg)] (Okamura et al., 2009). Furthermore, the specific accumulation of H12-(iopamidol)-liposomes at the injury site at the rat tail vein and jugular vein were identified using an explore Locus CT system (Okamura et al., 2009, 2010a). These results indicate that the H12-(ADP)-liposomes circulate in the bloodstream in a stable form until reaching the site of a vascular injury, and successfully augments hematostatic effects.

Retention in the blood is also an important factor in the evaluation of the hematostatic effects of H12-(ADP)-liposomes, because if the systemic half-life of the H12-(ADP)-liposome is too short, it cannot effectively function as a platelet substitute. From the viewpoint of future clinical applications, an allometric prediction of human pharmacokinetics based on data obtained from animal studies—so-called "animal scale-up"—is important for the determination of optimal doses and intervals (Izumi et al., 1996). In fact, we successfully predicted the blood retention properties of hemoglobin vesicles (HbV), the liposomal characteristics of which have similar characteristics in terms of liposomal structure to H12-(ADP)-liposomes. This

TABLE 2

Time course for the percentage of total detected ^{14}C radioactivity of ADP and metabolites derived from ^{14}C-ADP in urine after intravenous injection of ^{3}H- and ^{14}C-radiolabeled H12-(ADP)-liposomes at a dose of 10 mg lipids/kg to rats

Each value represents the mean ± S.D. (n = 4).

Time Course	Allantoin	ADP	Uric Acid	Hypoxanthine	Xanthine
6 h	89.7 ± 12.2	1.3 ± 1.2	N.D.	N.D.	N.D.
1 day	78.7 ± 13.3	16.0 ± 15.8	N.D.	N.D.	N.D.
3 day	71.8 ± 15.9	N.D.	N.D.	N.D.	11.2 ± 10.5
5 day	75.0 ± 20.8	N.D.	3.9 ± 3.4	N.D.	6.7 ± 5.9

N.D., not determined.

was accomplished using an allometric equation that is generally applied in animal scale-up studies to extrapolate the half-life of pharmaceuticals in humans. In the present study, we showed that the predicted half-life of H12-(ADP)-liposomes in humans would be approximately 96 hours (Fig. 5) using the above approach. The results obtained for a single-dose pharmacokinetic study of recombinant factor VIIa (rFVIIa), which is widely used as a hemostatic agent in clinical settings, showed that its half-life was 2–3 hours in patients with hemophilia (Lindley et al., 1994). These results indicate that H12-(ADP)-liposomes would be expected to adequately function as a hemostatic agent in the treatment of massive bleeding in humans.

Since H12-(ADP)-liposomes were developed as a synthetic platelet substitute, it is necessary to characterize the biodegradable properties of these particles, such as the determination of their metabolism and excretion pathways. Liposomes are generally captured and degraded by mononuclear phagocyte system (MPS) in the liver and spleen, such as by Kupffer cells and splenic macrophages (Kiwada et al., 1998). As expected, more than 10% of initial dose of the H12-(ADP)-liposomes were distributed to the liver and spleen (Fig. 2), which is in good agreement with a previous in vivo study using HbV (Sakai et al., 2001, 2004). In addition, an in vitro finding also reported that the specific uptake and degradation of HbV were observed only in macrophage cells but not in parenchymal and endothelial cells in the liver (Taguchi et al., 2009). Furthermore, linear pharmacokinetics were found for the H12-(ADP)-liposomes within the dose of 40 mg lipids/kg (Fig. 4). These results strongly suggest that the majority of the H12-(ADP)-liposomes are also scavenged and degraded by the MPS, such as by Kupffer cells or splenic macrophages, and that this process was not saturated at a dose of 40 mg lipids/kg. However, it was observed the different amount of ^{3}H and ^{14}C distribution in liver and spleen (Fig. 2). This was similar to our previous finding using HbV that inner hemoglobin was rapidly eliminated from organs to urine and outer lipid component (cholesterol) was delayed to eliminate from organs to feces (Taguchi et al., 2009).Therefore, the different elimination pathway would be related to the retention in liver and spleen. Further study will be needed in this point.

The findings herein also showed that most of the ADP in H12-(ADP)-liposomes was mainly metabolized to allantoin and excreted into the urine within 7 days after the injection of the ^{14}C, ^{3}H-labeled H12-(ADP)-liposomes (Fig. 3). It is well known that uric acid is the final metabolite of purines, such as adenosine 3′,5′-phosphate, in mammals. On the other hand, the principal metabolite of exogenous cyclic nucleotides in the rat is allantoin, and not uric acid (Coulson, 1976). Furthermore, another study showed that, in rats, hepatic uricase

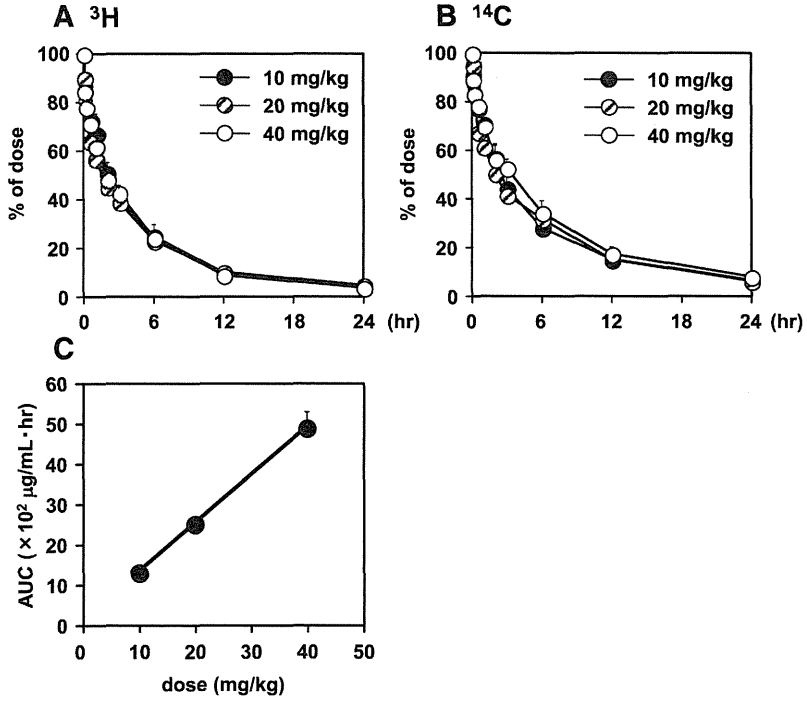

Fig. 4. Dose-dependent plasma concentration curve of (A) ^{3}H- and (B) ^{14}C-radiolabeled H12-(ADP)-liposome after intravenous injection at doses of 10, 20, and 40 mg lipids/kg to rats. Each point represents the mean ± S.D. (n = 4). (C) Relationship between the dose of H12-(ADP)-liposome and the area under the blood concentration-time curve. The linear regression of logarithmic values was calculated using the least-squares method (y = 98.33x+124.98, r^2 = 1)

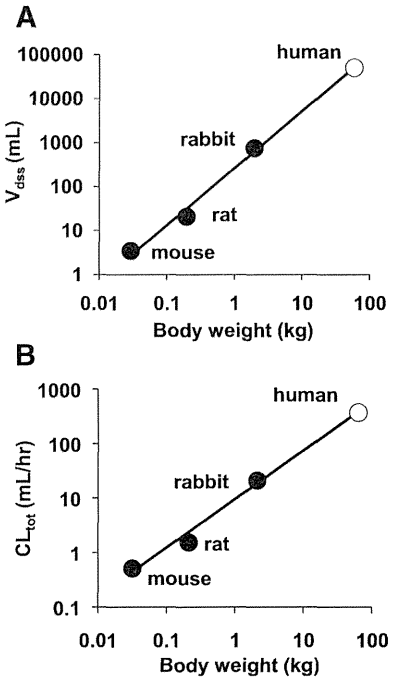

Fig. 5. Allometric relationships between body weight and distribution volume (V_{dss}) (A) and body weight and clearance (CL) (B). The linear regression of the logarithmic values was calculated using the least-squares method (A, $y = 257.71x^{1.2947}$, $r^2 = 0.965$; B, $y = 10.246x^{0.8928}$, $r^2 = 0.97$). The extrapolated human values based on a body weight of 70 kg (open circle) and the values from individual animals (gray circle) are also shown.

converts most of uric acid into allantoin, a form that allows it to be excreted in the urine more readily (Friedman and Byers, 1947). Taken together, these findings indicate that the ADP encapsulated by H12-(ADP)-liposome was completely metabolized and excreted into the urine even though ADP was encapsulated within liposome. However, ^{14}C radioactivity was not completely recovered until 7 days after ^{14}C-labeled H12-(ADP)-liposome administration. Although we could not explain the reason why the recovery of ^{14}C radioactivity was less than 100% at higher doses, it was suggested that a part of encapsulated ADP was used in the body as endogenous ADP.

The [^{3}H]cholesterol in H12-(ADP)-liposomes was mainly excreted into feces within 7 days after the injection of ^{3}H-labeled H12-(ADP)-liposomes. This result is in good agreement with the disposition of HbV, using HbV labeled with [^{3}H]cholesterol after an injection of HbV, which revealed that the majority of outer lipids component (cholesterol) was excreted via feces within 7 days (Taguchi et al., 2009). Kuipers et al. (1986) previously reported that cholesterol in vesicles reappear in the blood mainly as lipoprotein-cholesterol complexes after entrapment in Kupffer cells and should then be excreted in the bile after entrapment of the lipoprotein-cholesterol complex by hepatocytes. Therefore, a knowledge of whether the behavior of cholesterol as the lipid components of H12-(ADP)-liposome is the same as that of endogenous cholesterol after the metabolization of H12-(ADP)-liposome in the MPS would be highly desirable. On the other hand, we did not directly examine the disposition of the DPPC, DHSG, PEG-DSPE, and H12-PEG-Glu2C18 in H12-(ADP)-liposomes. Previous reports have shown that the phospholipids in liposomes are metabolized in the MPS and reused as cell membranes or are excreted into the bile (Dijkstra et al., 1985; Verkade et al., 1991). Therefore, it is also possible that phospholipids in H12-(ADP)-liposome are also metabolized and excreted in the same manner as the other liposome components, as mentioned above.

From the standpoint of biodegradable properties, it is also important to realize the possibility that H12-(ADP)-liposomes and components might accumulate in tissues, because it is well known that cholesterol is a risk factor for several diseases, including arteriosclerosis and hyperlipidemia. The findings reported herein indicate that both H12-(ADP)-liposomes and components derived from them disappeared from the bloodstream and organs within the 7 days after the injection of the H12-(ADP)-liposomes, indicating that H12-(ADP)-liposomes and components derived from them possess low accumulative properties. Therefore, H12-(ADP)-liposomes contain the appropriate components and have the potential for use as a synthetic platelet substitute, because they possess acceptable biodegradable properties.

Based on the present findings, we provide the first demonstration to show that the disposition of H12-(ADP)-liposomes and components derived from them occurs as follows. After being systemically administrated, the H12-(ADP)-liposomes are stable and circulate in an intact form in the circulation. As a result, some of the H12-(ADP)-liposomes would be specifically recruited at an injury site and would exert a pharmacological action, whereas the rest mainly are distributed to the liver and spleen, where they are degraded by the MPS. Finally, the encapsulated ADP and membrane components are eliminated mainly to the urine and feces, respectively, as final metabolites. In addition, our pharmacokinetic study, using different animal species, enabled us to predict that the half-life of H12-(ADP)-liposomes in humans is 96 hours. The above findings provide usable information for the development of the H12-(ADP)-liposomes for use as a platelet substitute.

Acknowledgments

The authors thank S. Katsuno and M. Arai at Waseda University for preparation of liposome samples.

Authorship Contributions

Participated in research design: Taguchi, Otagiri, Maruyama.
Conducted experiments: Taguchi, Ujihira, Ogaki, Fujiyama, Doi.
Contributed new reagents or analytic tools: Ikeda, Handa.
Performed data analysis: Taguchi, Ujihira, Watanabe.
Wrote or contributed to the writing of the manuscript: Taguchi, Okamura, Takeoka, Handa, Otagiri, Maruyama.

References

Agam G and Livne AA (1992) Erythrocytes with covalently bound fibrinogen as a cellular replacement for the treatment of thrombocytopenia. *Eur J Clin Invest* **22**:105–112.
Andrieux A, Hudry-Clergeon G, Ryckewaert JJ, Chapel A, Ginsberg MH, Plow EF, and Marguerie G (1989) Amino acid sequences in fibrinogen mediating its interaction with its platelet receptor, GPIIbIIIa. *J Biol Chem* **264**:9258–9265.
Blajchman MA (2003) Substitutes and alternatives to platelet transfusions in thrombocytopenic patients. *J Thromb Haemost* **1**:1637–1641.
Boxenbaum H (1984) Interspecies pharmacokinetic scaling and the evolutionary-comparative paradigm. *Drug Metab Rev* **15**:1071–1121.
Casals E, Verdaguer A, Tonda R, Galán A, Escolar G, and Estelrich J (2003) Atomic force microscopy of liposomes bearing fibrinogen. *Bioconjug Chem* **14**:593–600.
Coller BS, Springer KT, Beer JH, Mohandas N, Scudder LE, Norton KJ, and West SM (1992) Thromboerythrocytes. In vitro studies of a potential autologous, semi-artificial alternative to platelet transfusions. *J Clin Invest* **89**:546–555.
Coulson R (1976) Metabolism and excretion of exogenous adenosine 3′:5′-monophosphate and guanosine 3′:5′-monophosphate. Studies in the isolated perfused rat kidney and in the intact rat. *J Biol Chem* **251**:4958–4967.
Dijkstra J, van Galen M, Regts D, and Scherphof G (1985) Uptake and processing of liposomal phospholipids by Kupffer cells in vitro. *Eur J Biochem* **148**:391–397.
Friedman M and Byers SO (1947) Clearance of allantoin in the rat and dog as a measure of glomerular filtration rates. *Am J Physiol* **151**:192–197.
George SK, Dipu MT, Mehra UR, Singh P, Verma AK, and Ramgaokar JS (2006) Improved HPLC method for the simultaneous determination of allantoin, uric acid and creatinine in cattle urine. *J Chromatogr B Analyt Technol Biomed Life Sci* **832**:134–137.
Graham SS, Gonchoroff NJ, and Miller JL (2001) Infusible platelet membranes retain partial functionality of the platelet GPIb/IX/V receptor complex. *Am J Clin Pathol* **115**:144–147.

Hawiger J, Kloczewiak M, Bednarek MA, and Timmons S (1989) Platelet receptor recognition domains on the alpha chain of human fibrinogen: structure-function analysis. *Biochemistry* **28**: 2909–2914.

Heptinstall S, Johnson A, Glenn JR, and White AE (2005) Adenine nucleotide metabolism in human blood—important roles for leukocytes and erythrocytes. *J Thromb Haemost* **3**:2331–2339.

Izumi T, Enomoto S, Hosiyama K, Sasahara K, Shibukawa A, Nakagawa T, and Sugiyama Y (1996) Prediction of the human pharmacokinetics of troglitazone, a new and extensively metabolized antidiabetic agent, after oral administration, with an animal scale-up approach. *J Pharmacol Exp Ther* **277**:1630–1641.

Kiwada H, Matsuo H, and Harashima H (1998) Identification of proteins mediating clearance of liposomes using a liver perfusion system. *Adv Drug Deliv Rev* **32**:61–79.

Kloczewiak M, Timmons S, and Hawiger J (1982) Localization of a site interacting with human platelet receptor on carboxy-terminal segment of human fibrinogen gamma chain. *Biochem Biophys Res Commun* **107**:181–187.

Kloczewiak M, Timmons S, Lukas TJ, and Hawiger J (1984) Platelet receptor recognition site on human fibrinogen. Synthesis and structure-function relationship of peptides corresponding to the carboxy-terminal segment of the gamma chain. *Biochemistry* **23**:1767–1774.

Kuipers F, Spanjer HH, Havinga R, Scherphof GL, and Vonk RJ (1986) Lipoproteins and liposomes as in vivo cholesterol vehicles in the rat: preferential use of cholesterol carried by small unilamellar liposomes for the formation of muricholic acids. *Biochim Biophys Acta* **876**:559–566.

Lam SC, Plow EF, Smith MA, Andrieux A, Ryckwaert JJ, Marguerie G, and Ginsberg MH (1987) Evidence that arginyl-glycyl-aspartate peptides and fibrinogen gamma chain peptides share a common binding site on platelets. *J Biol Chem* **262**:947–950.

Levi M, Friederich PW, Middleton S, de Groot PG, Wu YP, Harris R, Biemond BJ, Heijnen HF, Levin J, and ten Cate JW (1999) Fibrinogen-coated albumin microcapsules reduce bleeding in severely thrombocytopenic rabbits. *Nat Med* **5**:107–111.

Lindley CM, Sawyer WT, Macik BG, Lusher J, Harrison JF, Baird-Cox K, Birch K, Glazer S, and Roberts HR (1994) Pharmacokinetics and pharmacodynamics of recombinant factor VIIa. *Clin Pharmacol Ther* **55**:638–648.

Marcus AJ, Broekman MJ, Drosopoulos JH, Islam N, Pinsky DJ, Sesti C, and Levi R (2003) Metabolic control of excessive extracellular nucleotide accumulation by CD39/ecto-nucleotidase-1: implications for ischemic vascular diseases. *J Pharmacol Exp Ther* **305**:9–16.

Nishikawa K, Hagisawa K, Kinoshita M, Shono S, Katsuno S, Doi M, Yanagawa R, Suzuki H, Iwaya K, and Saitoh D, et al. (2012) Fibrinogen γ-chain peptide-coated, ADP-encapsulated liposomes rescue thrombocytopenic rabbits from non-compressible liver hemorrhage. *J Thromb Haemost* **10**:2137–2148.

Okamura Y, Eto K, Maruyama H, Handa M, Ikeda Y, and Takeoka S (2010a) Visualization of liposomes carrying fibrinogen gamma-chain dodecapeptide accumulated to sites of vascular injury using computed tomography. *Nanomedicine* **6**:391–396.

Okamura Y, Katsuno S, Suzuki H, Maruyama H, Handa M, Ikeda Y, and Takeoka S (2010b) Release abilities of adenosine diphosphate from phospholipid vesicles with different membrane properties and their hemostatic effects as a platelet substitute. *J Control Release* **148**:373–379.

Okamura Y, Maekawa I, Teramura Y, Maruyama H, Handa M, Ikeda Y, and Takeoka S (2005) Hemostatic effects of phospholipid vesicles carrying fibrinogen gamma chain dodecapeptide in vitro and in vivo. *Bioconjug Chem* **16**:1589–1596.

Okamura Y, Takeoka S, Eto K, Maekawa I, Fujie T, Maruyama H, Ikeda Y, and Handa M (2009) Development of fibrinogen gamma-chain peptide-coated, adenosine diphosphate-encapsulated liposomes as a synthetic platelet substitute. *J Thromb Haemost* **7**:470–477.

Phillips DR, Charo IF, and Scarborough RM (1991) GPIIb-IIIa: the responsive integrin. *Cell* **65**: 359–362.

Rybak ME and Renzulli LA (1993) A liposome based platelet substitute, the plateletsome, with hemostatic efficacy. *Biomater Artif Cells Immobilization Biotechnol* **21**:101–118.

Sakai H, Horinouchi H, Tomiyama K, Ikeda E, Takeoka S, Kobayashi K, and Tsuchida E (2001) Hemoglobin-vesicles as oxygen carriers: influence on phagocytic activity and histopathological changes in reticuloendothelial system. *Am J Pathol* **159**:1079–1088.

Sakai H, Masada Y, Horinouchi H, Ikeda E, Sou K, Takeoka S, Suematsu M, Takaori M, Kobayashi K, and Tsuchida E (2004) Physiological capacity of the reticuloendothelial system for the degradation of hemoglobin vesicles (artificial oxygen carriers) after massive intravenous doses by daily repeated infusions for 14 days. *J Pharmacol Exp Ther* **311**:874–884.

Taguchi K, Urata Y, Anraku M, Maruyama T, Watanabe H, Sakai H, Horinouchi H, Kobayashi K, Tsuchida E, and Kai T, et al. (2009) Pharmacokinetic study of enclosed hemoglobin and outer lipid component after the administration of hemoglobin vesicles as an artificial oxygen carrier. *Drug Metab Dispos* **37**:1456–1463.

Takagi J, Petre BM, Walz T, and Springer TA (2002) Global conformational rearrangements in integrin extracellular domains in outside-in and inside-out signaling. *Cell* **110**:599–611.

Takeoka S, Teramura Y, Okamura Y, Handa M, Ikeda Y, and Tsuchida E (2001) Fibrinogen-conjugated albumin polymers and their interaction with platelets under flow conditions. *Biomacromolecules* **2**:1192–1197.

Verkade HJ, Derksen JT, Gerding A, Scherphof GL, Vonk RJ, and Kuipers F (1991) Differential hepatic processing and biliary secretion of head-group and acyl chains of liposomal phosphatidylcholines. *Biochem J* **275**:139–144.

Xiao T, Takagi J, Coller BS, Wang JH, and Springer TA (2004) Structural basis for allostery in integrins and binding to fibrinogen-mimetic therapeutics. *Nature* **432**:59–67.

Yamakawa N, Suemasu S, Watanabe H, Tahara K, Tanaka KI, Okamoto Y, Ohtsuka M, Maruyama T, and Mizushima T (2013) Comparison of pharmacokinetics between loxoprofen and its derivative with lower ulcerogenic activity, fluoro-loxoprofen. *Drug Metab Pharmacokinet* **28**:118–124.

Address correspondence to: Dr. Toru Maruyama, Department of Biopharmaceutics, Graduate School of Pharmaceutical Sciences, Kumamoto University, 5-1 Oe-honmachi, Kumamoto 862-0973, Japan. E-mail: tomaru@gpo.kumamoto-u.ac.jp

INTERFACE

基礎

ナノ粒子と血小板の相互作用
—完全人工系血小板代替物への応用を目指して—

岡村陽介[1*]　半田　誠[2]

[1] 東海大学創造科学技術研究機構 ナノ生体材料学研究室 講師
[2] 慶應義塾大学医学部 輸血細胞療法センター 教授

Yosuke Okamura[1*], MD
Assistant Professor, Nanobiomaterials Laboratory, Institute of Innovative Science and Technology, Tokai University, Hiratsuka, Japan

Makoto Handa[2], MD
Professor, Transfusion Medicine and Cell Therapy, School of Medicine, Keio University, Tokyo, Japan

* 第一著者連絡先:
〒259-1292 神奈川県平塚市北金目4-1-1 17号館401
Tel: 0463-58-1211 (Ex. 4877), Fax: 0463-50-2478, E-mail: y.okamura@tokai-u.jp

ABSTRACT

血小板は，血液凝固系と連動した巧妙かつ複雑な止血機構を有しており，これら全ての機能を人工系で模倣することは不可能といっても過言ではない．わが国では，厚生労働科学研究費の補助を受け［研究代表者：池田康夫教授（慶應義塾大学／現・早稲田大学）］，感染の危険性がなく長期間保存可能な完全人工系の血小板代替物の創製を目指し，世界に先駆けて開発してきた．具体的には，生体投与可能なナノ粒子に活性化血小板を認識できる分子（フィブリノーゲンγ鎖C末端ドデカペプチド，HHLGGAKQAGDV:H12）を担持させれば，それが損傷部位へ特異的に集積して血栓形成を誘導する起点となり，集積したナノ粒子によって出血部位を充填し止血能を補助できるとの発想に基づいて，極めて単純な血小板代替物を設計した．

はじめに

血小板は止血機構の中心的役割を果たす．現在，血小板の量的・質的異常により惹起される出血に対して信頼できる治療法は血小板輸血である．その供給量はここ5年間で急増しており[1]，先進医療に必須な血小板輸血の需要は将来も減少することはないと予想される．しかし，高齢化に伴う献血者数の低下や人口減少によって確保できる血小板製剤の絶対数の減少が予想されること，保存期間が日本では4日間と短く厳密な保存条件が必須であることから，緊急時等の供給体制が完全に整備されてないのが現状である．核酸増幅検査の導入により血液製剤の安全性は著しく向上したものの，未だにウイルス感染などのリスクは払拭されてはいない．さらに赤血球輸血とは異なり自己血輸血の推進が図れないため，今後の先進医療において，安定供給可能な血小板代替物の開発は当然目指すべき方向である[2]．

血小板の止血機構

血小板は通常血管内を流動しているが，血管損傷部位に露出した内皮下組織，特にコラーゲンを認識すると直ちに接着する．血小板の膜表面には，コラーゲンやそれに結合したフォンビレブランド因子（VWF）を認識する受容体が存在する．高血流条件下では，血小板膜糖蛋白質Ib（GPIb）がVWFを介したコラーゲンとの相互作用によって血小板が接着し，ローリング速度が緩やかになる[3]．次いで，コラーゲ